SoBRA
The Society of Brownfield Risk Assessment

SOCIETY OF BROWNFIELD RISK ASSESSMENT

Light Non-Aqueous Phase Liquid – Guidance Notes for their Assessment in Contaminated Land Scenarios in the UK

3. LNAPL MOBILITY SCREENING TOOL

Version 1.0

April 2023

SoBRA
The Society of Brownfield Risk Assessment

PUBLICATION

This series of reports and tools is published by the Society of Brownfield Risk Assessment (SoBRA). It presents work undertaken by a SoBRA sub-group composed of volunteers listed in the acknowledgments below. This publication is part of a series of work packages designed to address various issues in data collection and evaluating risks associated with non-aqueous phase liquid (NAPL).

NAPL mobility is an important metric in developing LNAPL conceptual site models (LCSM) and designing effective remediation. NAPL mobility is a function of the volume and footprint of the release as well as the properties of the NAPL, any other fluids present and the medium through which it potentially moves. This document provides a spreadsheet tool based on existing mobility equations from CL:AIRE, 2014 to provide a line of evidence as to whether NAPL in porous media is likely to be mobile. In addition, the tool has been used to provide example input data and graphical output to estimate the depth of LNAPL penetration below the water table and the critical thickness of LNAPL in a borehole, which will allow lateral mobility of selected LNAPL and lithology types. As set out in the text, it is imperative that users have read and understand the basis for the derivation of the tool and its limitations as described in the supporting text presented herein

The reports and tools are made available on the understanding that neither the contributors nor the publishing organisation are engaged in providing a specific professional service. Whilst every effort has been made to ensure the accuracy and completeness of the publications, no warranty as to fitness for purpose is provided or implied. Neither SoBRA nor the authors of the report accept any liability whatsoever for any loss or damage arising in any way from its use or interpretation, or from reliance on any views contained herein. Readers are advised to use the information contained herein purely as a guide for initial consultation about the topics and to take appropriate professional advice where necessary.

Published by the Society of Brownfield Risk Assessment www.sobra.org.uk. The Society of Brownfield Risk Assessment is a Registered Charity: No. 1180875.

ACKNOWLEDGMENTS

SoBRA wishes to thank the following individuals for their considerable assistance in the successful delivery of this document:

Working Group & Reviewers	**Employer**
Anna Hitchmough (lead author)	RSK Geosciences
Duncan Cartwright	Atkins Limited
Conor Armstrong	Avada Environmental
David Holmes	Geosyntec Consultants
Jonathan Parry	SLR Consulting Limited
Caroline Walker	WSP

SoBRA also wishes to thank the Executive Committee for their steer, encouragement and review.

CONTENTS

LIST OF FIGURES

LIST of APPENDICES

1 INTRODUCTION

The Society of Brownfield Risk Assessment (SoBRA) is a UK-based learned society that aims to:

- improve technical knowledge in risk-based decision-making related to land contamination applications; and
- enhance the professional status and profile of risk assessment practitioners.

The society has a number of working groups (termed "sub-groups") comprising volunteer SoBRA members working on particular aspects to help achieve these aims. This report presents one of several outputs of the non-aqueous phase liquid (NAPL) sub-group.

The technical aims of the sub-group are to:

- support technical excellence in the assessment, estimation and evaluation of risks associated with NAPL; and,
- encourage best practice by delivering practical advice to support decisions regarding the appropriate management of NAPL risks.

It should be noted from the outset it is not the intention of the sub-group or any of its deliverables to replicate or replace existing NAPL guidance. Instead, the overarching aim is to address gaps in current guidance, and to provide practical advice to SoBRA members when undertaking risk assessments at sites where NAPL could be or is present.

1.1 Evolution and overall strategy of the NAPL sub-group

The evaluation of contaminated land risk relies on understanding sub-surface processes. NAPL can be difficult to measure, meaning conceptual site models (CSM) may be data deficient. Following several requests from our members, SoBRA created the NAPL sub-group in 2019 with a call out to the SoBRA membership for volunteers to participate.

Once the group of volunteers was assembled, initial sub-group meetings identified and prioritised areas where existing NAPL UK risk assessment guidance was limited or would benefit from practical advice. As a result of this screening process, a series of seven working groups was formed, each tasked with producing a document or tool to address the identified need.

The overall approach developed by the sub-group to address NAPL risk assessment is summarised in Figure 1. The seven working groups cover all stages of risk assessment, ranging from establishing whether NAPL is likely to be present at a site or not, through to designing an appropriate remediation strategy. The position of this particular document within this strategy is highlighted in red.

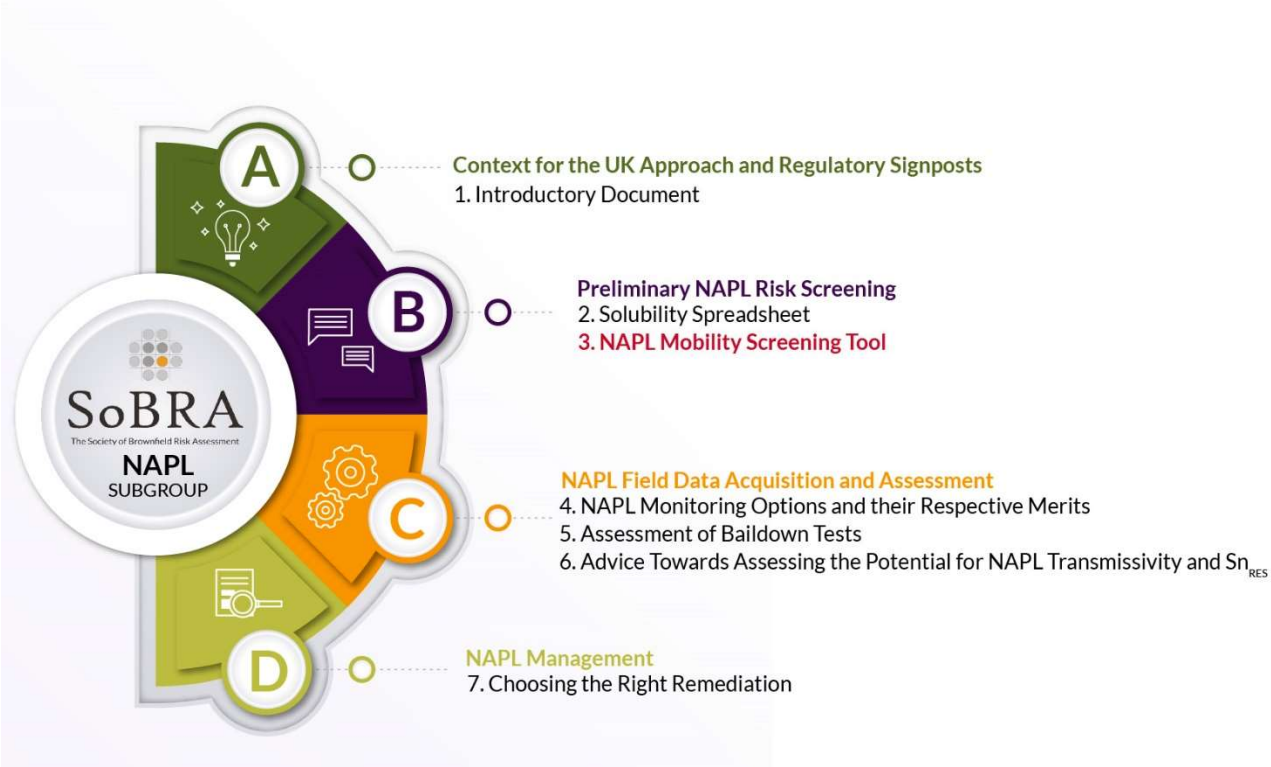

Figure 1 – Publication strategy for NAPL sub-group

1.2 Background

A migrating LNAPL body is expanding laterally or vertically into areas previously un-impacted by LNAPL. Mobile LNAPL exists above residual saturation levels such that it may be observed in monitoring wells. Mobile LNAPL has the *potential* to migrate, but not all mobile LNAPL is migrating LNAPL (ITRC, 2018).

LNAPL mobility is an important metric in developing LNAPL conceptual site models (LCSM) and designing effective remediation strategies. NAPL mobility is a function of the volume and footprint of the release as well as the properties of the LNAPL, any other fluids present and the medium through which it potentially moves.

This document relates to LNAPL in porous matrices only. Fractured matrices are not considered. DNAPL is not included.

LNAPL will be mobile when it has the energy to overcome resistance to its movement. The less viscous the LNAPL and the greater the driving head the more mobile it will be. Some 'residual' LNAPL, unable to overcome capillary forces, will remain immobile within pore spaces.

Equations for estimating whether LNAPL is mobile or not are provided in the literature. One easily accessible source is CL:AIRE, 2014. *An Illustrated Handbook of LNAPL Transport and Fate in the subsurface*, which includes equations for estimating the critical head of LNAPL in boreholes for lateral mobility and the penetration depth of LNAPL for a given head of LNAPL in formation above the water table.

The CL:AIRE document contains useful details of mobility principles not reproduced in this document.

1.3 Aims

The aims of this document are to:

- Provide explanation of the accompanying spreadsheets for the subset of equations described (from CL:AIRE, 2014), which provide a series of screening tools to estimate:
    - the depth of LNAPL penetration below the water table;
    - the critical thickness of LNAPL in a borehole which will allow lateral migration;
    - Darcy flux;
    - LNAPL hydraulic conductivity; and,
    - Lateral LNAPL velocity.
- Provide example input data and graphical output to estimate the depth of LNAPL penetration below the water table and the critical thickness of LNAPL in a borehole, which will allow lateral mobility of selected LNAPL and sediment types;
- Discuss which parameters mobility equations are most sensitive to as well as sources of uncertainty; and,
- Provide guidance on where to obtain suitable values for use in the equations.

2 KEY PRINCIPLES

2.1 Framework for NAPL mobility assessment and LCSM

Assessing LNAPL plume stability or mobility is a critical part of LNAPL risk assessment.

Because of the complexity of LNAPL behaviour, it is often helpful to follow a multiple lines of evidence approach to do this. Selected lines of evidence are listed below (adapted from Hawthorne, 2013):

- **Evaluation of LNAPL plume history and its life cycle stage** (e.g. is it an early, mid or late-stage plume as per API, 2018). Older plumes are more likely to be stable than newer LNAPL bodies and studies have shown that LNAPL bodies typically stabilize within 3 to 10 years of the original leak (Hawthorne and Kirkman, 2011);
- **Characterising the vertical and lateral footprint and extent of the LNAPL** (e.g. from ground investigation data, Photo Ionisation Detector (PID)/ Laser Induced Fluorescence (LIF) / Ultraviolet Fluorescence (UVF) surveys);
- **Using LNAPL dissolved and vapour phase data** to help delineate LNAPL plumes lateral and vertical extent, and any changes of this over time;
- **Understanding the effects of water table fluctuations and hydrogeology of the LNAPL setting**. This includes identifying whether the site fits into one of the four following LNAPL hydrogeological conditions (ITRC 2018):
    - Unconfined;
    - Confined;
    - Perched; or
    - Fractured / Complex.

  Illustrations of these conditions are summarised in Figure 2.
- **Understanding heterogeneity and preferential pathway effects**. Potential heterogeneous conditions or preferential pathways (e.g. utilities corridors) should be identified as these provide a greater degree of uncertainty in LNAPL assessments and mobility calculations; and,
- **Quantifying LNAPL mobility, recoverability, and migration potential.** For a well characterised LNAPL body which is in an unconfined setting, the LNAPL mobility and lateral migration potential can be quantified as a critical

well thickness for comparison to observed apparent LNAPL thicknesses in monitoring wells located at the plume front.

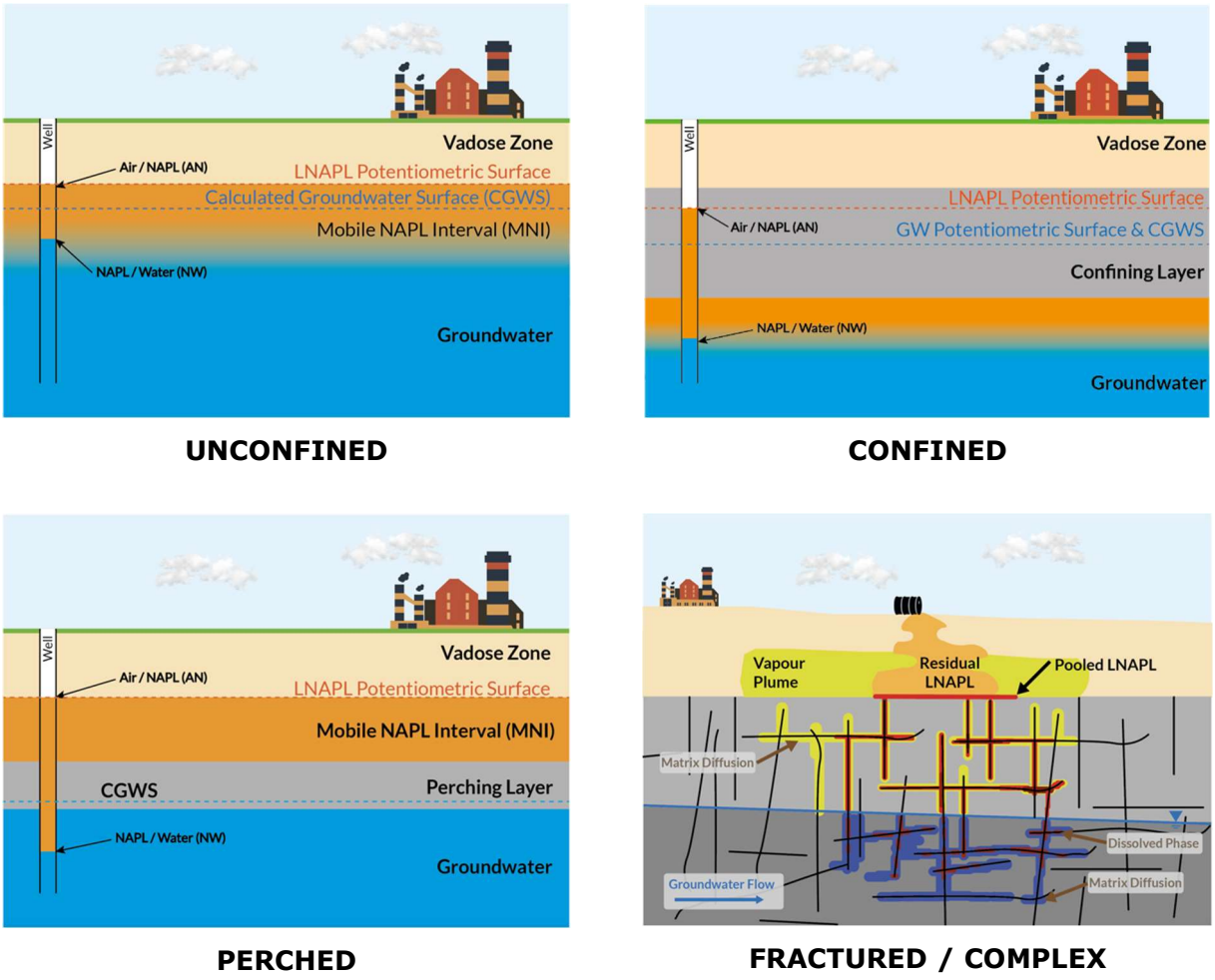

Figure 2 – Conceptual illustrations of the four LNAPL hydrogeological conditions (based on API, 2018 and CL:AIRE,2014)

The following sections provide the background to the series of calculation tools developed to help establish some of the above lines of evidence for evaluating an LNAPL plumes stability or mobility.

3 CALCULATING THE DEPTH OF LNAPL PENETRATION BELOW THE WATER TABLE

3.1 Introduction

A continuous source of LNAPL in a homogeneous granular unconfined aquifer will penetrate the water table until the pressure caused by the mass of LNAPL is matched by the buoyancy forces of the LNAPL and entry pressure the LNAPL needs to overcome to displace water from the pores of the aquifer matrix. The LNAPL will not penetrate vertically below the water table until displacement conditions are achieved, this displacement condition can be expressed mathematically by calculating the LNAPL height in the formation above the water table (the critical height) that will result in a penetration depth which is greater than zero.

Equations to calculate LNAPL penetration depth are provided in the accompanying spreadsheet given in Appendix 1. A brief description of the equations and the parameters they require follows.

The equation to calculate penetration depth is set out in the equation in Box 1 (CL:AIRE, 2014).

Box 1: Calculating penetration depth

$$h_p = \frac{\rho_N g h_n - \left(\frac{2\sigma cos\theta_A}{r}\right)}{\rho_W g}$$

Where:

h_P = penetration depth of LNAPL (m)

h_n = LNAPL height above water table in formation (m)

ρ_N = density of LNAPL ($kg.m^{-3}$)

ρ_W = density of groundwater ($kg.m^{-3}$)

θ_A = advancing contact angle through the wetting phase (°) [Refer to Section 3.4]

σ = interfacial tension between LNAPL and water ($N.m^{-1}$)

r = average pore throat radius (m)

g = Gravitational acceleration ($m.s^{-2}$)

As an example, potential methods to estimate average pore throat radius are given in Box 2.

Box 2: Estimating average pore throat radius

Method 1: Nelson, 2009 equation

$k \approx 4.48 d^2 \emptyset^2$

Therefore

$d \approx \sqrt{\left(\frac{k}{4.48\emptyset^2}\right)}$ / 1000

and

$r = {}^{d}/_{2}$

where:

d = pore throat diameter (m)

r = pore throat radius (m)

k = intrinsic permeability (microdarcies[1])

$\emptyset$ = porosity (-)

Notes

[1]one darcy is equivalent to 0.831 m.day^{-1}

Method 2: USEPA, 2017 equation

r=0.2D

where:

r = pore throat radius (m)

D = mean particle diameter (m)

Notes

A suitable estimate of mean particle diameter may be obtained from literature or estimated from a particle size distribution analysis, e.g., d50.

3.2 Example calculation of critical LNAPL heights for selected sediment types

In order to demonstrate the importance and sensitivity of the soil or sediment type (its grain size) and the fluid type to the LNAPL penetration depth, the graph in Figure 3 has been produced for a variety of LNAPL and sediments using the literature values given in Appendix 2. The graphs illustrate the theoretical critical height of LNAPL in the

formation at which the LNAPL starts to penetrate the water table i.e. the height at which the penetration depth is greater than zero (h_P>0). The critical height was derived iteratively by varying the LNAPL height above water table in formation (h_N) until the penetration depth exceeded zero. Note that critical height can also be interchangeably described as critical head. If this critical head is not exceeded (h_P<0) then LNAPL is likely to stop moving at some point in in the unsaturated zone of the overlying formation and will not penetrate below the water table.

Please note that the graphs are provided as examples only, and it is up to the user to ensure that the literature values they choose fit the LCSM at their site.

The LNAPL types considered were:

- petrol;
- diesel;
- kerosene; and,
- cable/lube oil.

The sediment types considered were:

- fine silt;
- coarse silt;
- very fine sand;
- fine sand;
- medium sand;
- coarse sand;
- very coarse sand; and,
- fine gravel.

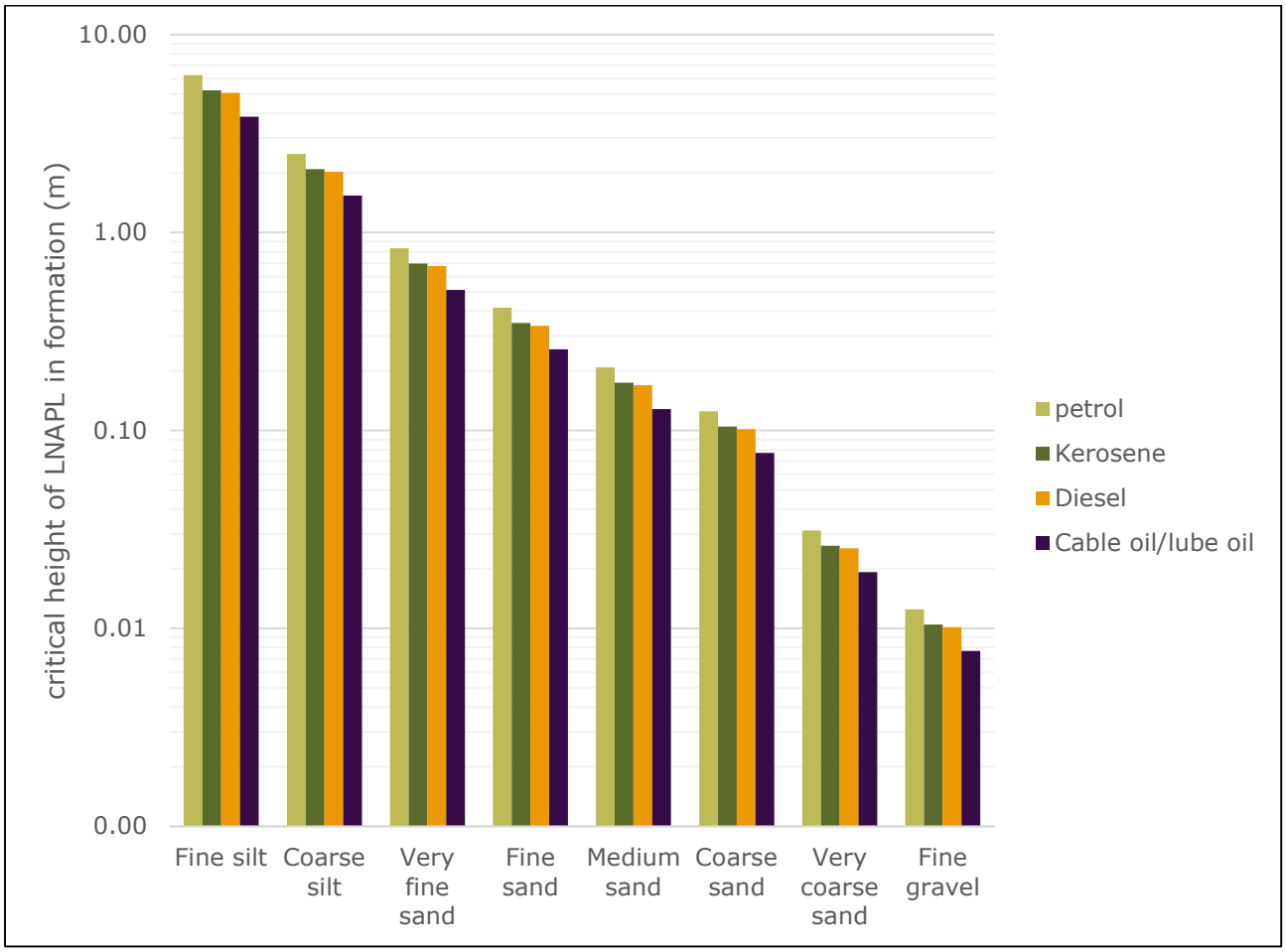

Figure 3 – Graph of critical LNAPL height in selected sediments for vertical penetration into water table

3.3 Sensitivity analysis

As given in Appendix 4, sensitivity analysis was carried out using the default parameter. Each parameter was varied in turn to change the output of the equation. A comprehensive multi-parameter analysis was not carried out. The results are presented in Figure 4 as a Tornado diagram. The figure indicates that the height above the water table, the average pore throat radius and LNAPL density influence the output of this equation. The density of the groundwater, interfacial tension between LNAPL and water, and advancing contact angle through the wetting phase are insensitive in this equation.

It was, however, noted that for finer grained sediments with smaller pore-throat radii, the advancing contact angle becomes increasingly important. The advancing contact angle became increasingly sensitive in sediments with a pore-throat radius of 0.00001 m (10 µm), which is characteristic of a silt (Nelson, 2009) and intersects with zero at a pore throat radius of approximately 0.5 µm.

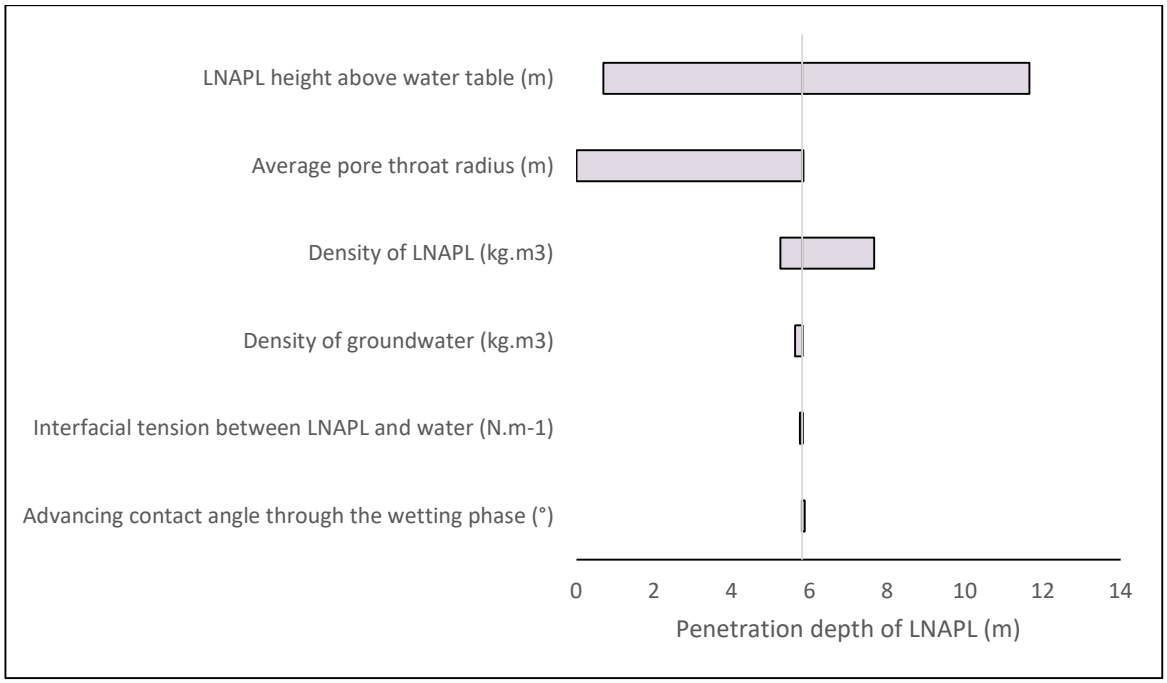

Figure 4 – Parameter sensitivity for the penetration depth of LNAPL

Only three of the six parameters materially affect the equation output.

3.4 Uncertainty

Figure 3 has been produced as an example, but the LNAPL conceptual site model at every site is different. Therefore, the values estimated by the graphs should not be directly applied to sites as a generic standard. It is up to the practitioner to ensure that input parameters applied are appropriate for site specific conditions. A guide to field and laboratory methods of determining some of the key parameters is given in API, 2001. Other options include use of appropriate literature values or mathematical estimation.

There are very little published data available for some of the input parameters for the critical LNAPL height (h_n). Of particular note was the paucity of data available for the advancing contact angle (θ_A) through the wetting phase used in the equation estimating the penetration depth of LNAPL. However, as shown in Figure 4, when varying the angle between zero and 70 degrees (the typical range quoted in CL:AIRE, 2014 for LNAPL), it made very little difference to the calculated penetration depth and therefore a discretionary value of 30 degrees was used to produce the example graph.

3.5 Using the vertical penetration spreadsheet tool in LNAPL risk assessment

The spreadsheet tool provided in Appendix 1 calculates how deep a vertical column of NAPL will penetrate below the water table. It is envisaged that it could be used during a preliminary stage of LNAPL risk assessment in the following scenarios:

- During a desk-based review to assess whether there are any deeper receptors present below the groundwater level that could be at risk of being impacted by the vertically penetrating LNAPL, for example underlying sensitive bedrock (e.g. superficial drift over principal bedrock aquifers) or underlying higher permeability geological layers such as basal gravel units or chalk hardgrounds.
- As part of site investigation scoping and design to identify vertical characterisation requirements (e.g. proposed borehole investigation depths and well response zone designs).
- To calibrate or sense check existing field observation data (such as visual staining profiles, or volatile organic compound (VOC) soil headspace profiles using a PID) to determine whether the calculated penetration depth reflects site investigation findings. A broad correlation between calculated depth and field observation would provide greater confidence in the LCSM.

3.5.1 Example calculation

A real-world example of using the spreadsheet tool is included in Box 3 below.

Box 3: An illustration of an LNAPL penetration depth calculation

A buried petrol delivery pipe was found to have been leaking to ground for some time. The pipe was located at a depth of 0.3 m below ground. A desk-based review of the site setting identified the geology as Alluvium comprising coarse sands and gravels to 8 m depth overlying Chalk bedrock (a principal aquifer and within an SPZ). Groundwater in existing wells elsewhere on site was recorded at 4m depth within the Alluvium. The spreadsheet tool was used to calculate the expected LNAPL penetration depth below the water table, to determine whether the underlying Chalk aquifer was at risk from the LNAPL.

This site information indicated a potential LNAPL height in the unsaturated zone of 3.7 m (i.e. 4 m depth to groundwater – depth to the pipe of 0.3 m). Literature values for fluid properties, advancing contact angle; and pore throat radius calculated from anticipated average grain size (for a coarse sand) were used.

An extract of the tool is reproduced below:

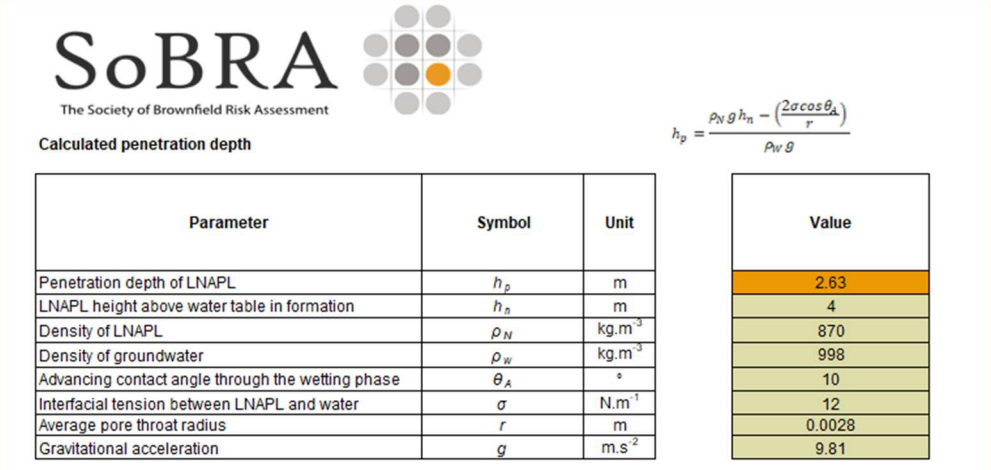

SoBRA
The Society of Brownfield Risk Assessment

Calculated penetration depth

$$h_p = \frac{\rho_N g h_n - \left(\frac{2\sigma\cos\theta_A}{r}\right)}{\rho_W g}$$

Parameter	Symbol	Unit	Value
Penetration depth of LNAPL	h_p	m	2.63
LNAPL height above water table in formation	h_n	m	4
Density of LNAPL	ρ_N	$kg.m^{-3}$	870
Density of groundwater	ρ_W	$kg.m^{-3}$	998
Advancing contact angle through the wetting phase	θ_A	°	10
Interfacial tension between LNAPL and water	σ	$N.m^{-1}$	12
Average pore throat radius	r	m	0.0028
Gravitational acceleration	g	$m.s^{-2}$	9.81

The calculation recorded an LNAPL penetration depth of 2.63 m below the groundwater level, indicating the LNAPL would likely penetrate though the Alluvium deposit to a depth of approximately 6.63 m below ground level, but would not likely extend into the underlying Chalk aquifer, present below 8 m.

This data was used to assist the scoping of the subsequent ground investigation, with separate well installation designs to enable further assessment of lateral LNAPL mobility conditions and potential recovery in the Alluvium and assessment of dissolved phase quality within the deeper Chalk bedrock.

4 SCREENING FOR THE LIKELIHOOD OF LATERAL LNAPL MIGRATION

4.1 Introduction

Once LNAPL has penetrated the water table and vertical migration has stopped, it will migrate laterally until it reaches equilibrium conditions with lateral confining pressures.

4.2 Critical thickness for lateral migration to commence

The critical thickness that LNAPL in a monitoring borehole must reach in order to continue to migrate laterally within an aquifer below the groundwater table is given in Box 4.

Box 4: Calculating critical thickness for lateral migration

The equation for calculating the critical thickness of LNAPL in a borehole before lateral migration occurs within groundwater is given below (CL:AIRE, 2014):

$$h_{NBH,critical} = \left(\frac{\sigma_{NW}}{1 - \frac{\rho_N}{\rho_W}} - \frac{\sigma_{AN}}{\frac{\rho_N}{\rho_W}} \right) \frac{h_D}{\sigma_{AW}}$$

where:

$h_{NBH,critical}$ = thickness of LNAPL in a well/borehole needed to exceed pore entry pressure (m)

σ_{NW} = interfacial tension between LNAPL and groundwater ($N.m^{-1}$)

σ_{AN} = surface tension of LNAPL ($N.m^{-1}$)

σ_{AW} = surface tension of groundwater ($N.m^{-1}$)

ρ_N = density of LNAPL ($kg.m^{-3}$)

ρ_W = density of groundwater ($kg.m^{-3}$)

h_D = displacement pressure head i.e., height of capillary fringe (m)

Equations to calculate LNAPL critical thickness are provided in the accompanying spreadsheet given in Appendix 1.

4.3 Example graph

The graph in Figure 5 has been produced for a variety of LNAPL and sediments using the literature values given in Appendix 2.

Please note that the graphs are provided as *examples only*, and it is up to the user to ensure that the literature values they choose fit the LCSM at their site.

The LNAPL types considered were:

- petrol;
- diesel;
- kerosene; and
- cable/lubrication oil.

The sediment types considered were;

- fine silt;
- coarse silt;
- very fine sand;
- fine sand;
- medium sand;
- coarse sand;
- very coarse sand; and
- fine gravel.

There are multiple equations and methodologies in the scientific literature for determining the height of the capillary fringe. One such approximation to the height of the capillary fringe was estimated as described in Box 5. There is an accompanying simple spreadsheet tool for estimating capillary height from average pore size given in Appendix 3.

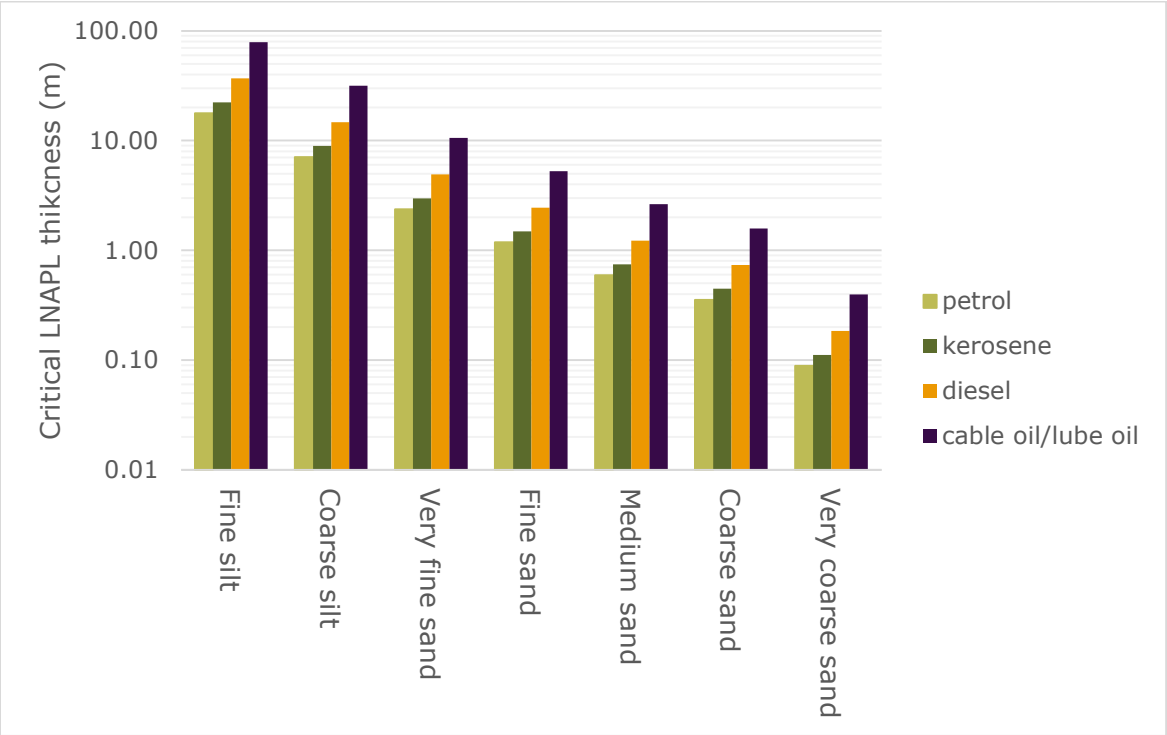

Figure 5 – Graph of critical LNAPL height in formation saturated sediments (i.e. below the water table) for lateral movement

Box 5: Calculating the capillary fringe (after USEPA (2017)

$$h_p = (\frac{0.15}{r})/100$$

where:

h_p = displacement pressure head i.e., height of capillary fringe (m)

r = average pore throat radius (m)

4.4 Sensitivity analysis

As shown in Appendix 4, a sensitivity analysis was carried out. Each parameter was varied in turn to change the output of the equation. A multi-parameter analysis was not carried out. The results are presented in Figure 6 as a Tornado diagram. The Figure indicates that the displacement pressure head, the density of the LNAPL, the interfacial tension between the LNAPL and groundwater and surface tension of the groundwater are the most sensitive parameters. The equation is relatively insensitive to the surface tension of the LNAPL and the density of the groundwater. Note: groundwater density inland can be assumed to be a fixed value, but may increase in coastal sites due to the present of salt.

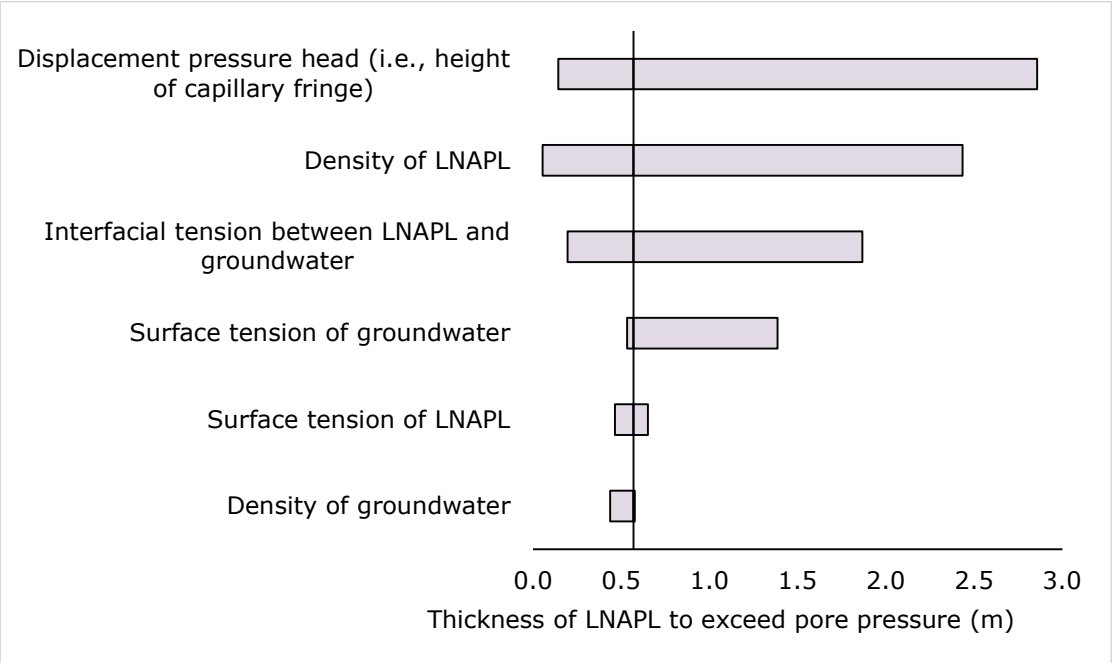

Figure 6 – Parameter sensitivity for the LNAPL thickness in a well to exceed pore pressure

The capillary fringe height, LNAPL density, interfacial tension and surface tension of groundwater are the most sensitive parameters.

4.5 Uncertainty

Graphs have been produced for illustrative purposes, but the LNAPL conceptual site model at every site is different. Therefore, the values predicted by the graphs cannot be directly applied to sites as a generic standard. It is up to the practitioner to ensure that input parameters and conceptual assumptions applied are appropriate for site specific conditions. A guide to field and laboratory methods of determining some of the key parameters is given in API, 2001. Other options include use of appropriate literature values or mathematical estimation.

For example, the height of the capillary fringe is rarely measured on a routine basis and seldom reported in literature. It is up to the user to decide whether to measure the capillary fringe or estimate it theoretically; either from literature (for example, figure 5 in *API methods for determining Inputs to environmental petroleum hydrocarbon mobility and recovery models*, API, 2001) or by estimating using an equation such as the one given in Box 5.

Measurement of the capillary fringe is practically difficult. The capillary fringe is a function of the soil water characteristic curve (SWCC). To calculate the SWCC, a number of techniques can be used which are outlined in Tuller et al., (2004).

4.6 Using the lateral migration spreadsheet tool in LNAPL risk assessment

The spreadsheet tool provided in Appendix 1 calculates the minimum LNAPL thickness in a well that is required for the LNAPL to be able to move through the ground, for the specific soil or sediment type present. This calculation can be used to compare to measured apparent in-well LNAPL thickness, on suitably well characterised sites, to determine whether the LNAPL is mobile on the NAPL body scale and able to migrate, and to aid with risk management decisions.

For example, it can be used at initial risk screening stage to provide a risk--based threshold at an early stage of assessment, or it can be used as a validation or remedial target on sites subject to LNAPL mass recovery.

4.6.1 Example Calculation

A real-world example of using the spreadsheet tool is included in Box 6 below.

Box 6: An illustration of an LNAPL lateral migration calculation

A refuelling leak of diesel at a bulk fuel depot resulted in a loss of product to ground in superficial soils comprising coarse sands. Remedial works installed several LNAPL recovery wells across the site and in situ LNAPL skimming took place for a number of years until minimal recovery rates were achieved. Following completion of remediation, persistent measurable LNAPL was still recorded in one well on-site as illustrated in the graph:

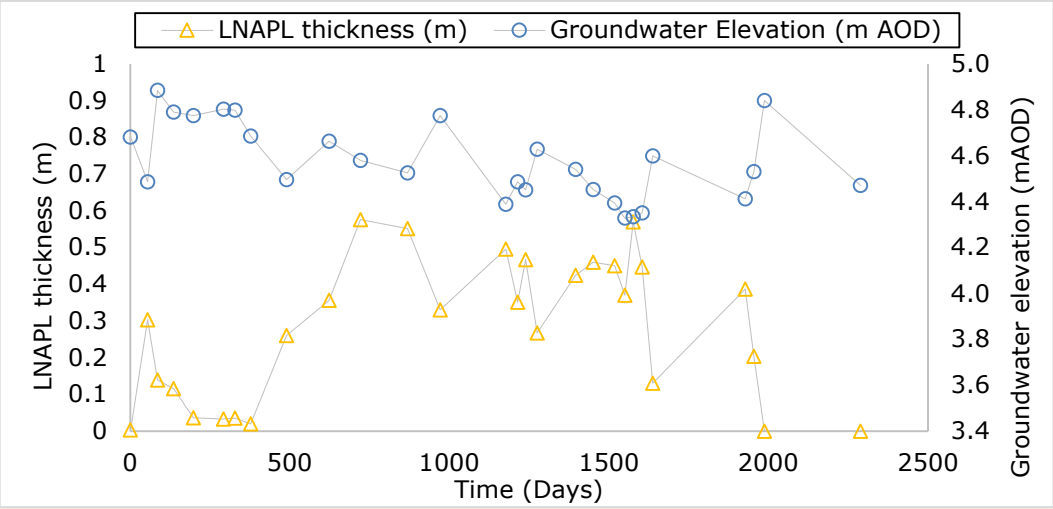

mAOD is metres above ordnance datum

Following an extended period of monitoring to evaluate LNAPL accumulations with changes in groundwater elevation, the critical well thickness was calculated using the spreadsheet tool. This derived a critical well thickness of 0.76 m needed for lateral NAPL migration.

An extract of the tool is reproduced below:

SoBRA
The Society of Brownfield Risk Assessment

Calculated critical thickness

$$h_{NBH,critical} = \left(\frac{\sigma_{NW}}{1 - \frac{\rho_N}{\rho_W}} - \frac{\sigma_{AN}}{\frac{\rho_N}{\rho_W}} \right) \frac{h_D}{\sigma_{AW}}$$

Parameter	Symbol	Unit	Value
Thickness of LNAPL in a well to exceed pore entry pressure	$h_{NBH,critical}$	m	0.76
Interfacial tension between LNAPL and groundwater	σ_{NW}	$N.m^{-1}$	0.05
Surface tension of LNAPL	σ_{AN}	$N.m^{-1}$	0.03
Surface tension of groundwater	σ_{AW}	$N.m^{-1}$	0.07
Density of LNAPL	ρ_N	$kg.m^{-3}$	870
Density of groundwater	ρ_W	$kg.m^{-3}$	998
Displacement pressure head (i.e., height of capillary fringe)	hd	m	0.15

Comparison of the measured in well thickness recorded a maximum LNAPL thickness of 0.58 m on site, which was consistently below the 0.76 m critical NAPL thickness calculated. This was used to inform an assessment that the LNAPL present on site was not mobile at a NAPL body scale[1] and was unlikely to migrate in the future.

[1] LNAPL not mobile at a "NAPL body scale" [see page 17] means the NAPL body as a whole unit is not mobile and able to expand in areal extent or migrate along the flow path at a macro scale. Localised pockets of NAPL within the body may still be mobile and able to move within the NAPL body, but migration at the front of the body will not occur (see glossary for a definition of terms).

5 VELOCITY OF MOVEMENT

5.1 Introduction

Once LNAPL has exceeded the pore pressure and starts moving laterally, the velocity can be estimated (see Box 7).

Box 7: Calculating the velocity of lateral migration

$$V_n = \frac{q_n}{\eta_{eff}} = \frac{q_n}{\eta S_n}$$ (CL:AIRE, 2014)

where:

v_n = velocity of LNAPL (m.s^{-1})

η_{eff} = NAPL filled effective soil porosity (-)

S_n = LNAPL saturation of pore space (-)

η = total soil porosity (-)

q_n = Darcy flux for LNAPL (m.s^{-1}), which can be calculated using the equation:

$$q_n = K_n i_n$$

where:

i_n= LNAPL gradient (-)

K_n = LNAPL hydraulic conductivity (m.s^{-1}), which can be calculated with:

$$K_n = K_{w,sat} \frac{\rho_n \mu_w}{\rho_w \mu_n} k_m$$

where:

$K_{w,sat}$ = Groundwater hydraulic conductivity for fully saturated conditions (m.s^{-1})

ρ_N = density of LNAPL (kg.m^{-3})

ρ_W = density of groundwater (kg.m^{-3})

μ_n = dynamic viscosity of LNAPL (N s.m^{-2} (1))

μ_w = dynamic viscosity of groundwater (N s.m^{-2} (1))

k_m = LNAPL relative permeability (-)

Notes

(1) viscosity is often reported in cP. To convert: cP = 0.001 N s.m^{-2} = 0.001 Pa s

Equations to calculate LNAPL velocity are provided in the accompanying spreadsheet given in Appendix 1.

5.2 Sensitivity analysis

Tornado plots showing the relative sensitivity of parameters is given in the figures below.

The sensitivity of LNAPL velocity to variations in Darcy flux, NAPL filled effective porosity, NAPL saturation and total porosity are given in Figure 7. They illustrate that velocity is most sensitive to Darcy flux. NAPL filled effective porosity is the next most sensitive parameter.

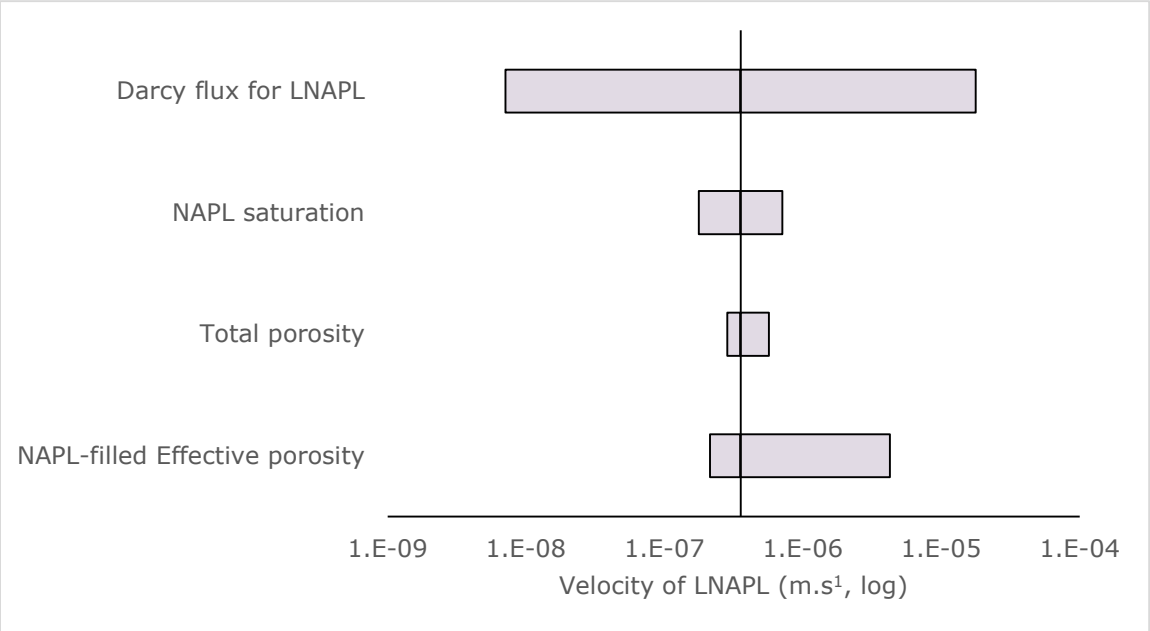

Figure 7 – Parameter sensitivity for the velocity of LNAPL

The relative sensitivity of Darcy flux to LNAPL hydraulic conductivity and LNAPL gradient are shown in Figure 8. The Darcy flux is most sensitive to LNAPL hydraulic conductivity.

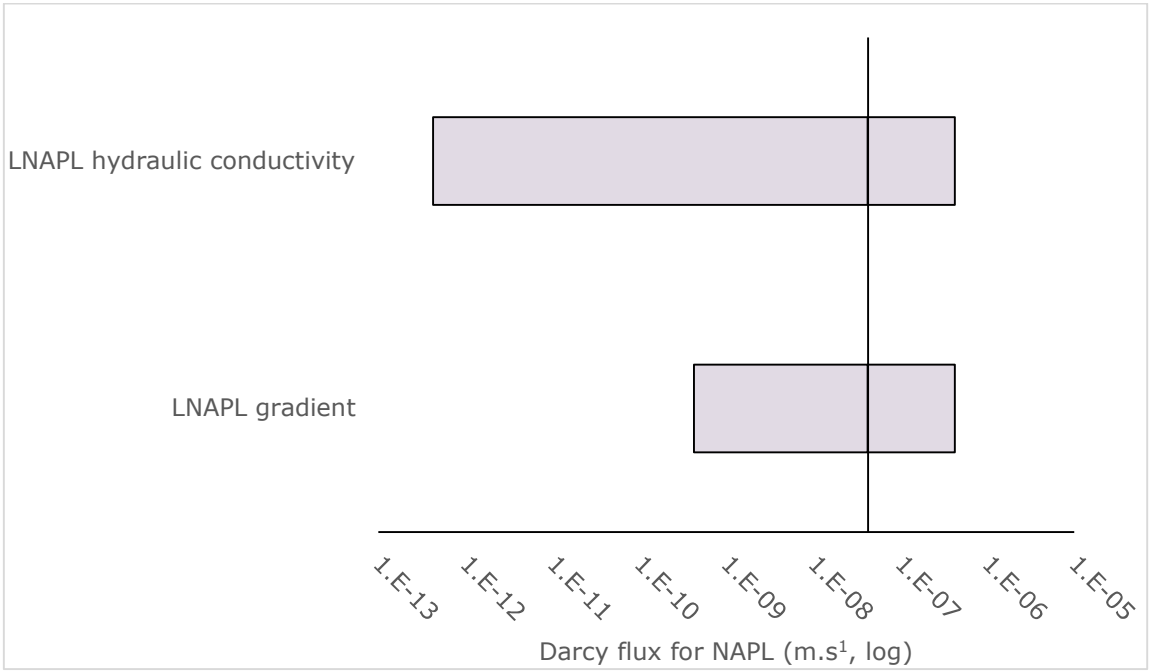

Figure 8 – Parameter sensitivity for the Darcy flux for LNAPL

Figure 9 shows that the hydraulic conductivity of the groundwater saturated medium and dynamic viscosity of the LNAPL are the main influencing factors in determining the magnitude of LNAPL velocity.

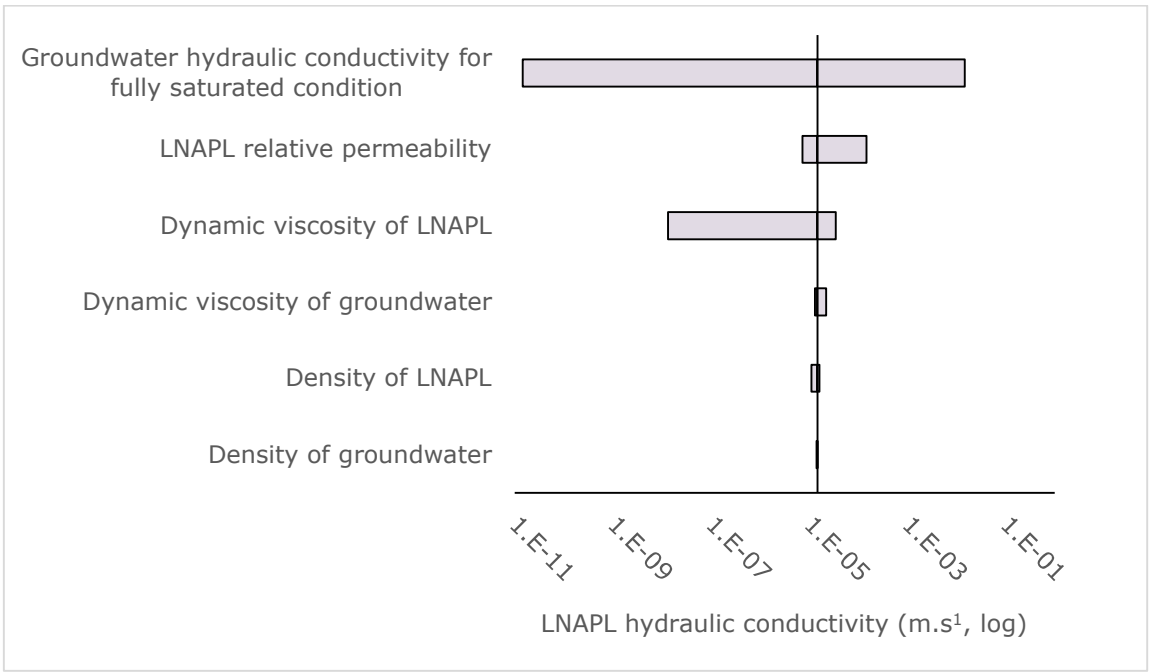

Figure 9 – Parameter sensitivities for LNAPL hydraulic conductivity

5.3 Uncertainty

It is up to the practitioner to ensure that input parameters and conceptual assumptions applied are appropriate for site specific conditions. A guide to field and laboratory methods of determining some of the key parameters is given in API, 2001. Other options include use of appropriate literature values or mathematical estimation.

Accurate application of the velocity equations in Box 5 may be problematic due to a sparsity of field data. Some data, such as LNAPL viscosity can be measured routinely in a laboratory and sometimes in the field. Other data such as LNAPL relative permeability and LNAPL-filled effective porosity are far more challenging and require specialised laboratory testing equipment and interpretation to provide a result.

In the absence of site specific or appropriate literature values, it is recommended to consider the range of minimum and maximum probable values to provide a range of outputs, along with a robust sensitivity analysis on a site-specific basis. Example parameters and their range can be found in Appendix 4.

6 COMMENTARY ON DATA SOURCES

Each site will have specific values which may be specific to each individual well. Some parameters are routinely measured, for example, hydraulic conductivity and a representative range was found in the literature. However, others, such as the average pore throat radius, are less commonly measured in environmental applications. Therefore, professional judgement should be applied in all cases with the parameter sensitivity guides used to inform the practitioner as to which parameters should be prioritised for measurement.

Within the sensitivity analysis each equation was initially solved using default values from CL:AIRE, 2014. A range of values was then sought from the existing literature to provide a range of realistic values to be environmentally relevant and used in the sensitivity assessments. The values used are presented and referenced in Appendix 4.

For some parameters, for example the LNAPL density, the lowest value of a pure component (hexane) was used as minimum, with the maximum value being informed by professional judgement. In reality, the value most appropriate to use at a given site will be site specific.

The surface tension of groundwater is usually well defined, however, to account for cases where there have been uncontrolled releases of other liquids, which affect this parameter, the value was varied accordingly. The surface tension of groundwater can be decreased by co-contaminants sometimes found at LNAPL-impacted sites. The sensitivity analysis considered a concurrent spill of butanol and its effects on surface tension.

The literature source values of average pore throat radius used in the sensitivity analysis as a minimum value was around 180 times smaller than the default value provided in the CL:AIRE, 2014 document. The CL:AIRE document used an assumed value of 100 µm which was more relevant to geology more commonly, but not always, encountered in LNAPL site investigations.

Equations to estimate the height of the capillary fringe, based on mean particle size have been provided. This can be routinely estimated from site investigations where particle size distribution analysis has been carried out.

7 REFERENCES

American Petroleum Institute (API), 2001. Methods for determining Inputs to environmental petroleum hydrocarbon mobility and recovery models, API publication 4711

API, 2004. Interactive LNAPL Guide, Version 2.0, July 2004. (free download at https://www.api.org/oil-and-natural-gas/environment/clean-water/ground-water/lnapl/interactive-guide)

API, 2018. Soil and Groundwater Research Bulletin 18: Managing Risk at LNAPL Sites - Frequently Asked Questions

Barnes, K., 2010. Soil Mechanics: Principles and practice. 3rd ed. Published by Palgrave Macmillan

CL:AIRE, 2014. An Illustrated Handbook of LNAPL Transport and Fate in the Subsurface.

Fetter, C.W., 1994. Applied Hydrogeology. 3rd ed. New York

Freeze and Cherry, 1979. Groundwater. New Jersey

Griffin, 1925. Density of a Lubricating oil at Temperatures from -40 deg to 20 deg C. Industrial and Engineering Chemistry, Vol 17, 11 pp 1157-1156

Hawthorne, J.M., 2013. LNAPL Body Stability, Part 1: Lines of Evidence. Applied NAPL Science Review. Volume 3, Issue 4

Hawthorne, J.M. and Kirkman, A., 2011. Residual, Mobile and Migrating LNAPL. Applied NAPL Science Review. Volume 1. Issue 10

Interstate Technology & Regulatory Council (ITRC), 2018. LNAPL Site Management: LCSM Evolution, Decision Process, and Remedial Technologies. LNAPL-3. Interstate Technology & Regulatory Council, LNAPLs Team, Washington, D.C. www.itrcweb.org

Johansen, E.M., 1924. The Interfacial Tension between Petroleum Products and Water. Industrial and Engineering Chemistry, Vol 16,2 pp132-135

Nelson, 2009. Pore-throat sizes in sandstones, tight sandstones, and shales. AAPG Bulletin, v. 93, no. 3 (March 2009), pp. 329–340

Tuller, M., Or, D. and Hillel, D., 2004. Retention of water in soil and the soil water characteristic curve. Encyclopaedia of Soils in the Environment, 4, pp.278-289

United States Environmental Protection Agency (US EPA), 2017. Documentation For EPA's Implementation Of The Johnson And Ettinger Model To Evaluate Site Specific Vapor Intrusion Into Buildings, USEPA Office Of Superfund Remediation And Technology Innovation.

APPENDIX 1

Spreadsheet tool

(Refer Appendix 1 Version 1 April 2023.xls)

APPENDIX 2

Data used for examples

VALUES USED TO PRODUCE EXAMPLE GRAPHS

1. LNAPL PROPERTIES

LNAPL type	Density of LNAPL (ρ_N)		
	literature values ($g.cm^{-3}$)	source	value used in graph ($kg.m^{-3}$)
petrol	0.67-0.8	CL:AIRE 2014, Table 2.1, pg. 4	735
diesel	0.87	CL:AIRE 2014, Table 2.1, pg. 4	870
kerosene	0.81	CL:AIRE 2014, Table 2.1, pg. 4	810
cable oil/lubrication oil	0.945	Griffin 1925	945

LNAPL type	Interfacial tension between LNAPL and water (σ)		
	literature values ($mN.m^{-1}$)	source	value used in graph ($N.m^{-1}$)
petrol	52	CL:AIRE 2014, Table 2.1, pg. 4 at 15 °C	0.052
diesel	50	CL:AIRE 2014, Table 2.1, pg. 4 at 15 °C	0.05
kerosene	47-49	CL:AIRE 2014, Table 2.1, pg. 4 at 15 °C	0.048
cable oil/lubrication oil	33.2-49.2	Johansen, 1924. mid point at 25 °C	0.0412

LNAPL type	Advancing contact angle through the wetting phase (θ_A)		
	literature values (°)	source	value used in graph
petrol	30	CL:AIRE, 2014. pg 89 petrol in glaciofluvial sand and gravel, pg 94 petrol in chalk	30
diesel	10	EA, 2014. pg 93 diesel in granite	30
kerosene	-	no info available	30
cable oil/lubrication oil	-	no info available	30

LNAPL type	Surface tension of LNAPL (σ_{AN})		
	literature values ($mN.m^{-1}$?)	source	value used in graph ($N.m^{-1}$)
petrol	18.6	API database for leaded gasoline at 15°C	0.0186
diesel	22.8-34.5	API database for diesel at 15°C	0.028433333
kerosene	31.2	API database for Jet A/Jet A-1l at 15°C	0.0312
cable oil/lubrication oil	7.9	API database for lubricating oil (Hydraulic, Esso XD3-10) at 15°C	0.0079

LNAPL type	Density of LNAPL (ρN)		
	literature values ($g.cm^{-3}$)	source	value used in graph ($kg.m^{-3}$)
petrol	0.67-0.8	CL:AIRE 2014, Table 2.1, pg. 4	735
diesel	0.87	CL:AIRE 2014, Table 2.1, pg. 4	870
kerosene	0.81	CL:AIRE 2014, Table 2.1, pg. 4	810
cable oil/lubrication oil	0.945	Griffin 1925	945

2. SEDIMENT PROPERTIES

Lithology type	Average pore throat radius (r)		
	Value used in graph (cm)	source	comment
Fine silt	0.0002	Fetter, 1994	calculated from grain diameter
Coarse silt	0.0005		
Very fine sand	0.0015		
Fine sand	0.003		
Medium sand	0.006		
Coarse sand	0.01		
Very coarse sand	0.04		
Fine gravel	0.10		

Lithology type	Displacement pressure head (i.e., height of capillary fringe) [hd]	
	value used in graph (m)	source
Fine silt	7.5	Calculated from average pore throat diameters using the equation in Box 4
Coarse silt	3	
Very fine sand	1	
Fine sand	0.5	
Medium sand	0.25	
Coarse sand	0.15	
Very coarse sand	0.0375	
Fine gravel	0.015	

APPENDIX 3

Spreadsheet for estimating capillary fringe

(Refer Appendix 3 Version 1 April 2023.xls)

APPENDIX 4

Data used for sensitivity analysis

Table A4-1 Depth of LNAPL penetration below the water table

CALCULATED PARAMETER	EQUATION	PARAMETER	UNIT	SYMBOL	DEFAULT VALUE
Depth of LNAPL penetration below the water table	$h_p = \frac{\rho_N g h_n - \left(\frac{2\sigma cos\theta_A}{r}\right)}{\rho_W g}$	**Penetration depth of LNAPL**	**m**	h_P	**5.81**
		LNAPL height above water table	m	h_N	8
		Density of LNAPL	kg.m^{-3}	ρ_N	729
		Density of groundwater	kg.m^{-3}	ρ_W	998
		Advancing contact angle through the wetting phase	°	θ_A	30
		Interfacial tension between LNAPL and water	N.m^{-1}	σ	0.018
		Average pore throat radius	m	r	0.0001
		Gravitational acceleration	m.s^{-2}	g	9.81

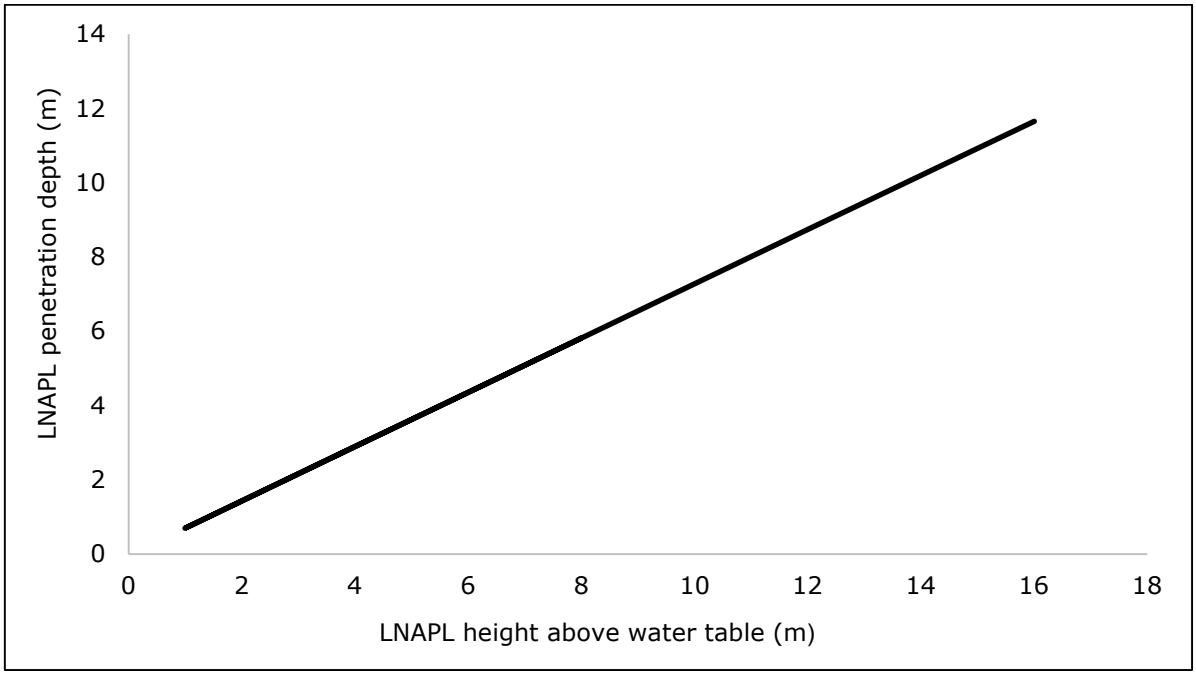

Figure A4-1. Sensitivity of LNAPL penetration depth to LNAPL height above the water table

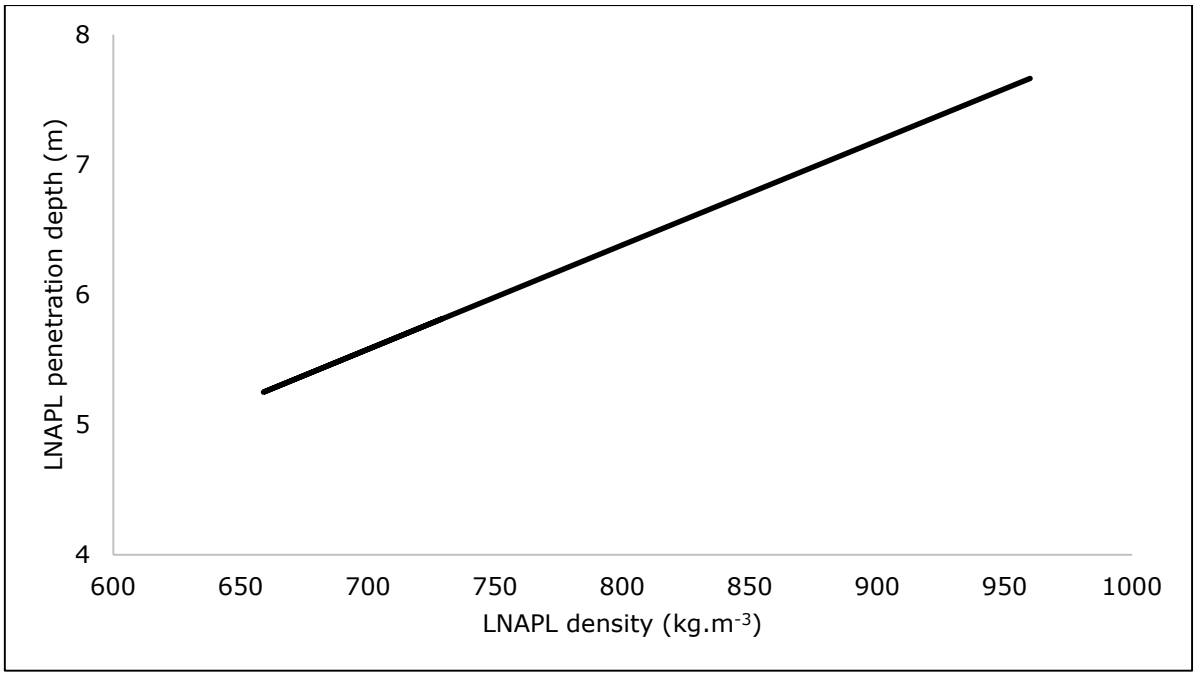

Figure A4-2. Sensitivity of LNAPL penetration depth to LNAPL density

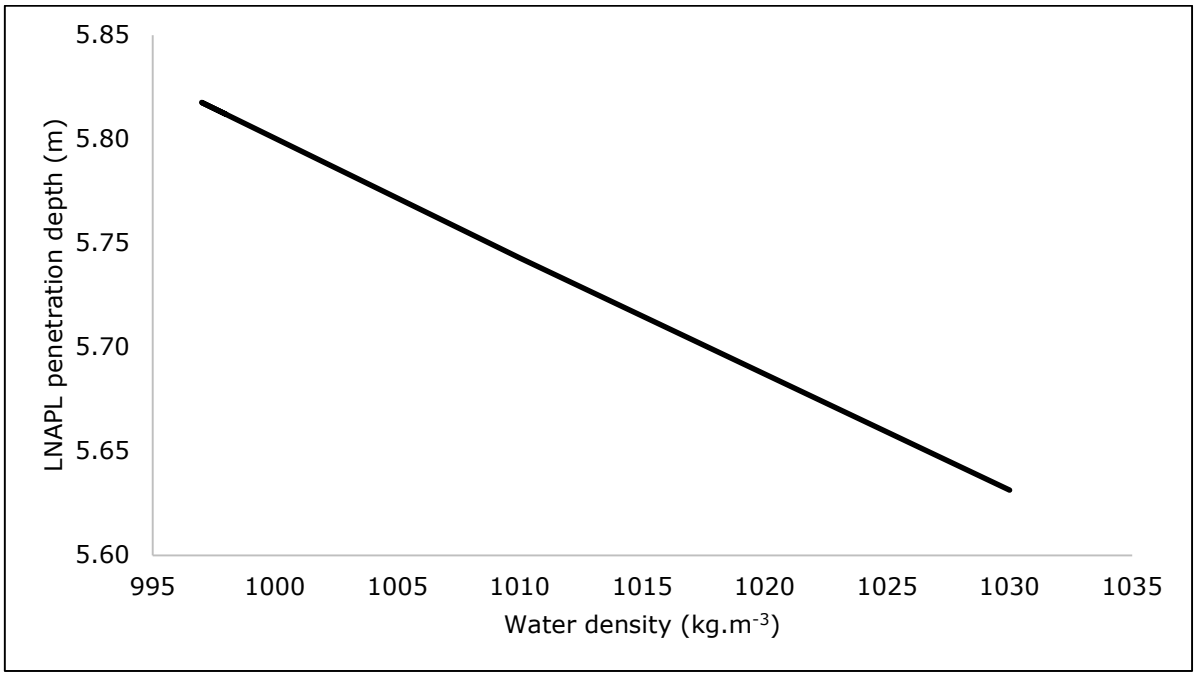

Figure A4-3. Sensitivity of LNAPL penetration depth to water density

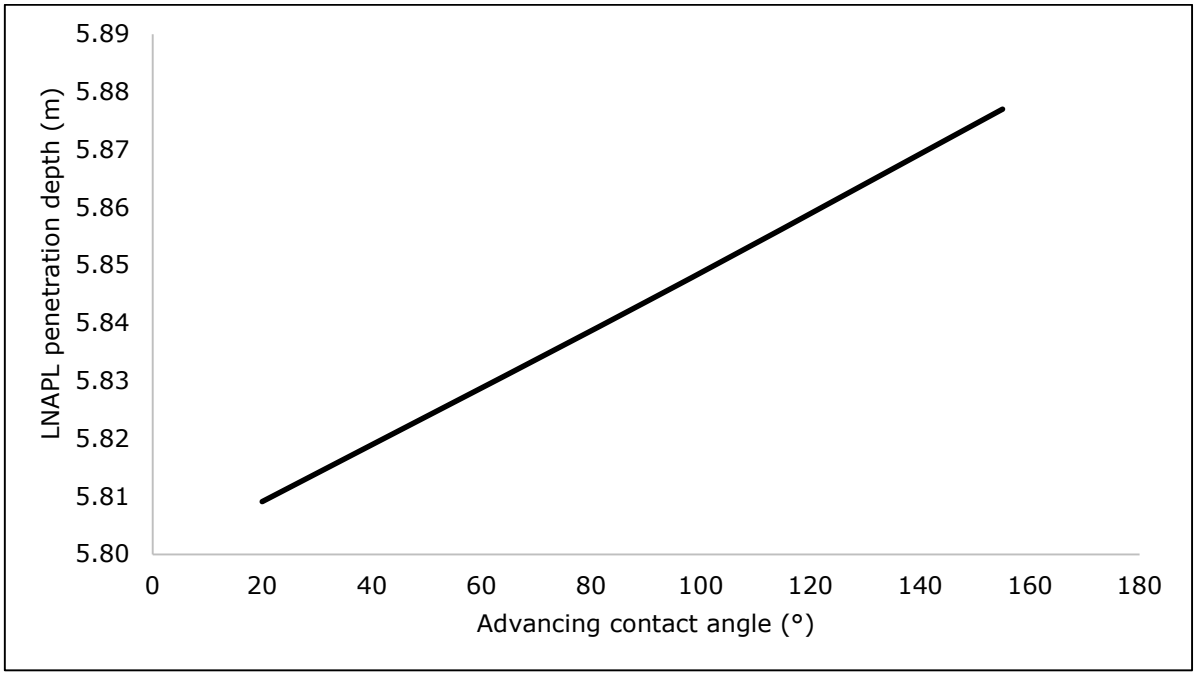

Figure A4-4. Sensitivity of LNAPL penetration depth to advancing contact angle

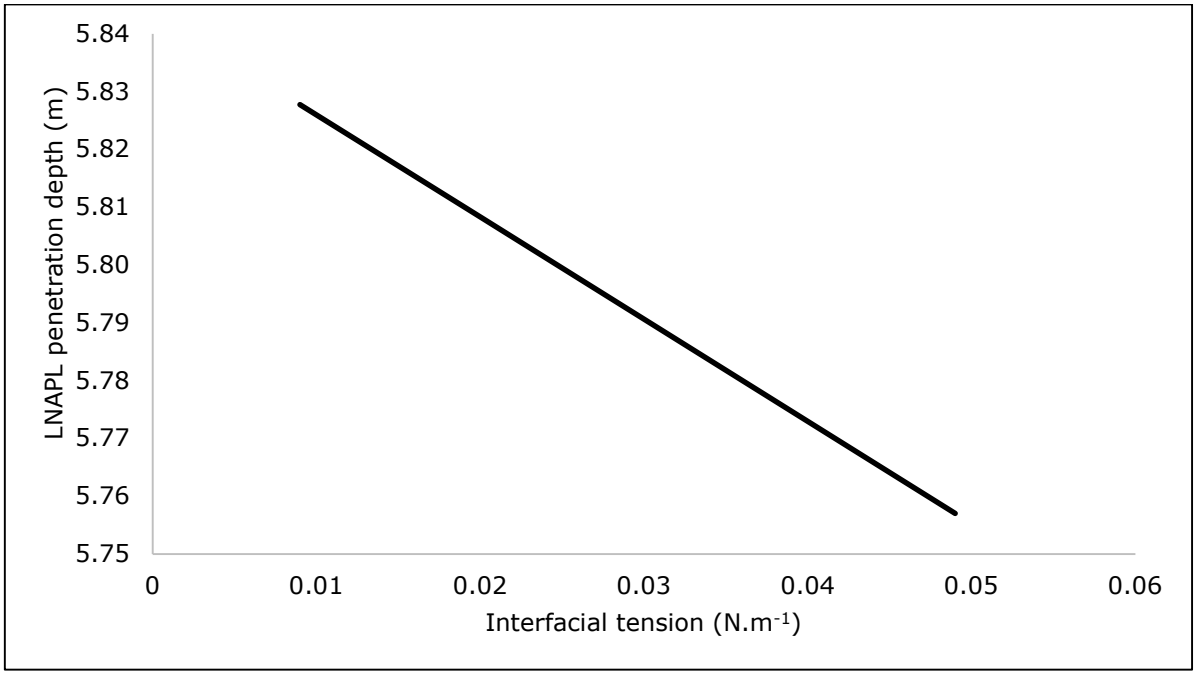

Figure A4-5. Sensitivity of LNAPL penetration depth to interfacial tension

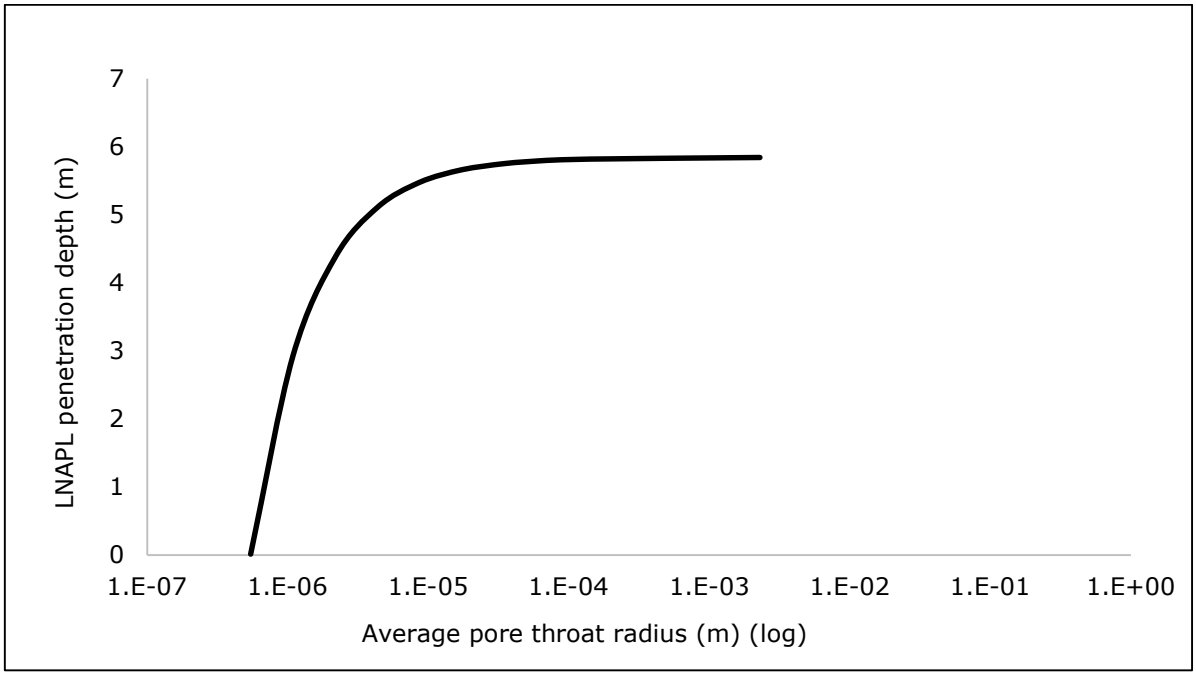

Figure A4-6. Sensitivity of LNAPL penetration depth to average pore throat density

Table A4-2 LNAPL lateral spread

CALCULATED PARAMETER	EQUATION	PARAMETER	UNIT	SYMBOL	DEFAULT VALUE
LNAPL lateral spread	$h_{NBH,critical} = \left(\frac{\sigma_{NW}}{1-\frac{\rho_N}{\rho_W}} - \frac{\sigma_{AN}}{\frac{\rho_N}{\rho_W}}\right)\frac{h_D}{\sigma_{AW}}$	**Thickness of LNAPL in a well/borehole to exceed pore entry pressure**	**m**	$\boldsymbol{h_{NBH,critical}}$	**0.57**
		Interfacial tension between LNAPL and	N.m^{-1}	σ_{NW}	0.02
		Surface tension of LNAPL	N.m^{-1}	σ_{AN}	0.03
		Surface tension of groundwater	N.m^{-1}	σ_{AW}	0.07
		Density of LNAPL	kg.m^{-3}	ρ_N	867
		Density of groundwater	kg.m^{-3}	ρ_W	998
		Displacement pressure head (i.e., height of capillary fringe)	m	h_D	0.4

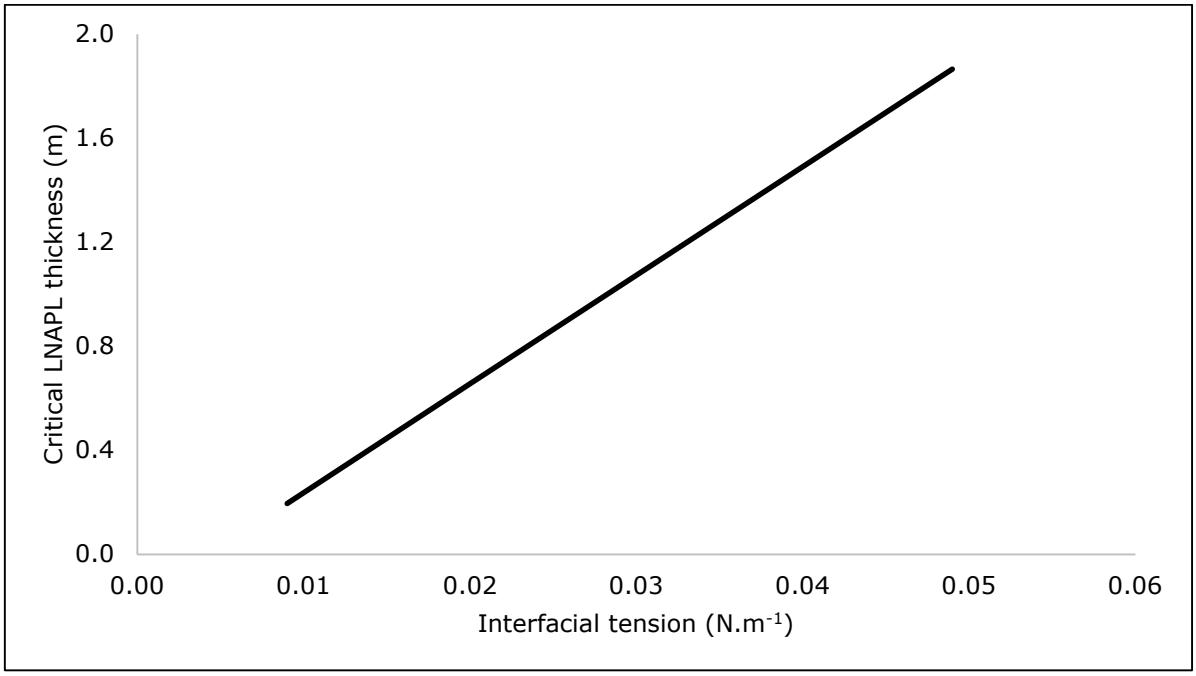

Figure A4-7. Sensitivity of LNAPL critical thickness to interfacial tension

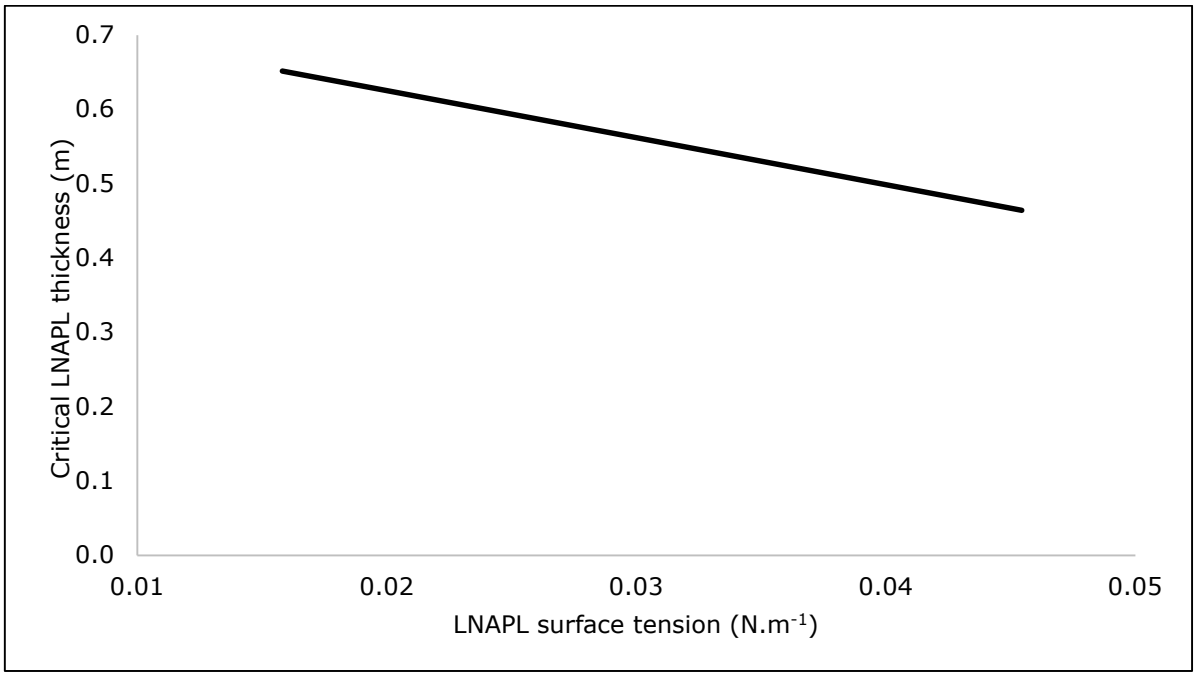

Figure A4-8. Sensitivity of LNAPL critical thickness to LNAPL surface tension

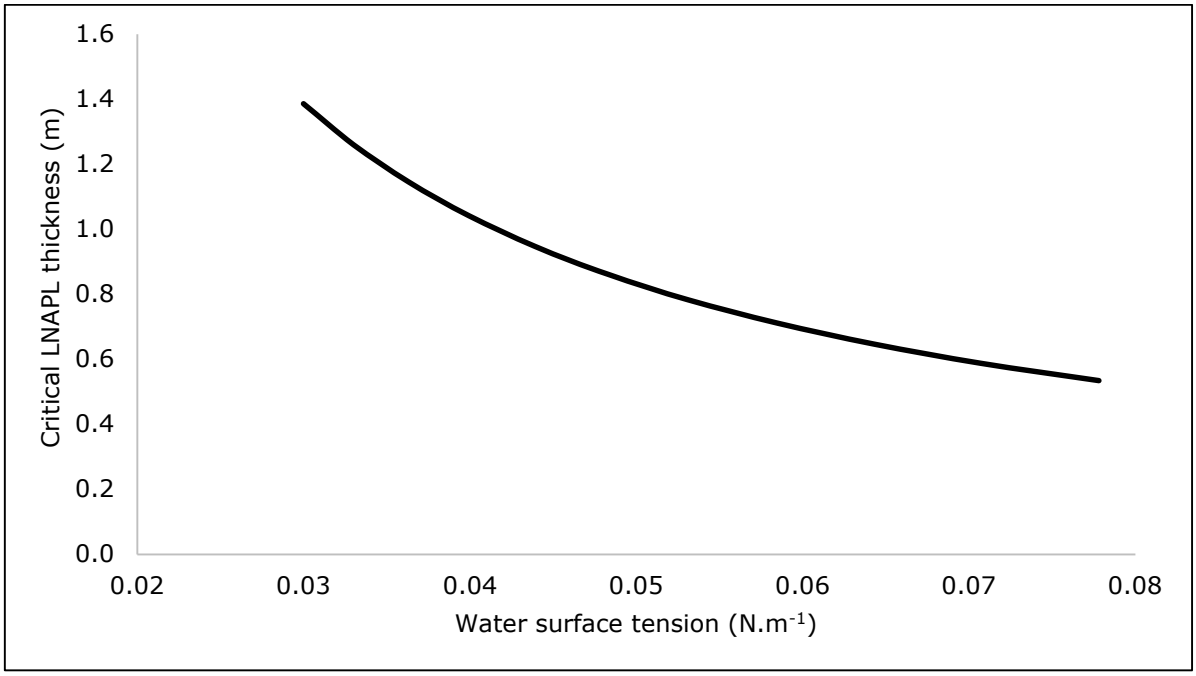

Figure A4-9. Sensitivity of LNAPL critical thickness to water surface tension

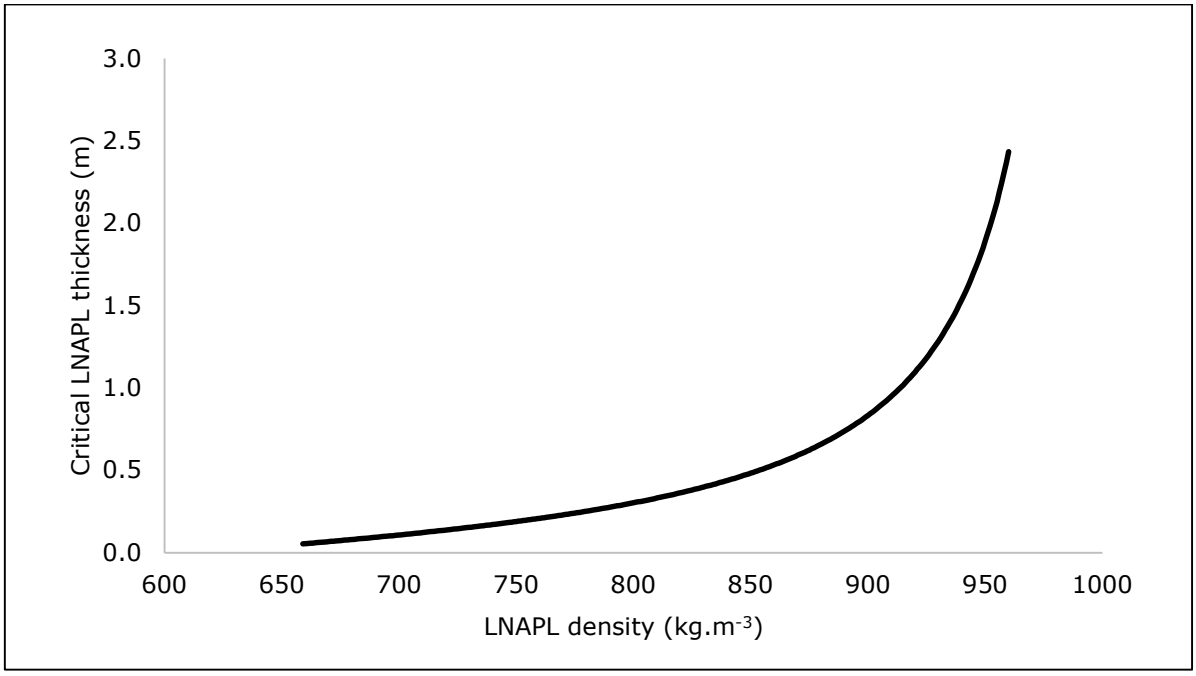

Figure A4-10. Sensitivity of LNAPL critical thickness to LNAPL density

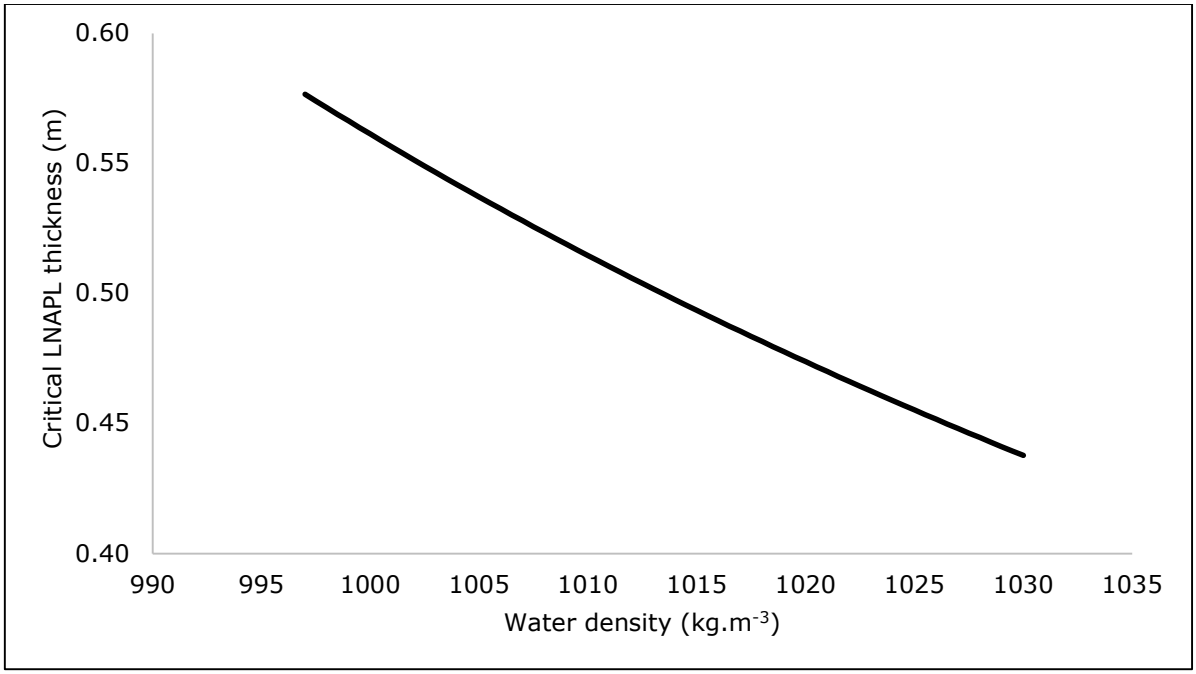

Figure A4-11. Sensitivity of LNAPL critical thickness to water density

Figure A4-12. Sensitivity of LNAPL critical thickness to capillary fringe height

Table A4-3 LNAPL migration rate (1)

CALCULATED PARAMETER	EQUATION	PARAMETER	UNIT	SYMBOL	DEFAULT
Migration rate	$V_N = \frac{q_N}{\eta_{Neff}}$	**Velocity of LNAPL**	$m.s^{-1}$	v_N	3.6E-07
		Darcy flux for LNAPL	$m.s^{-1}$	q_N	4.3E-08
		NAPL-filled effective porosity	-	η_{Neff}	1.2E-01

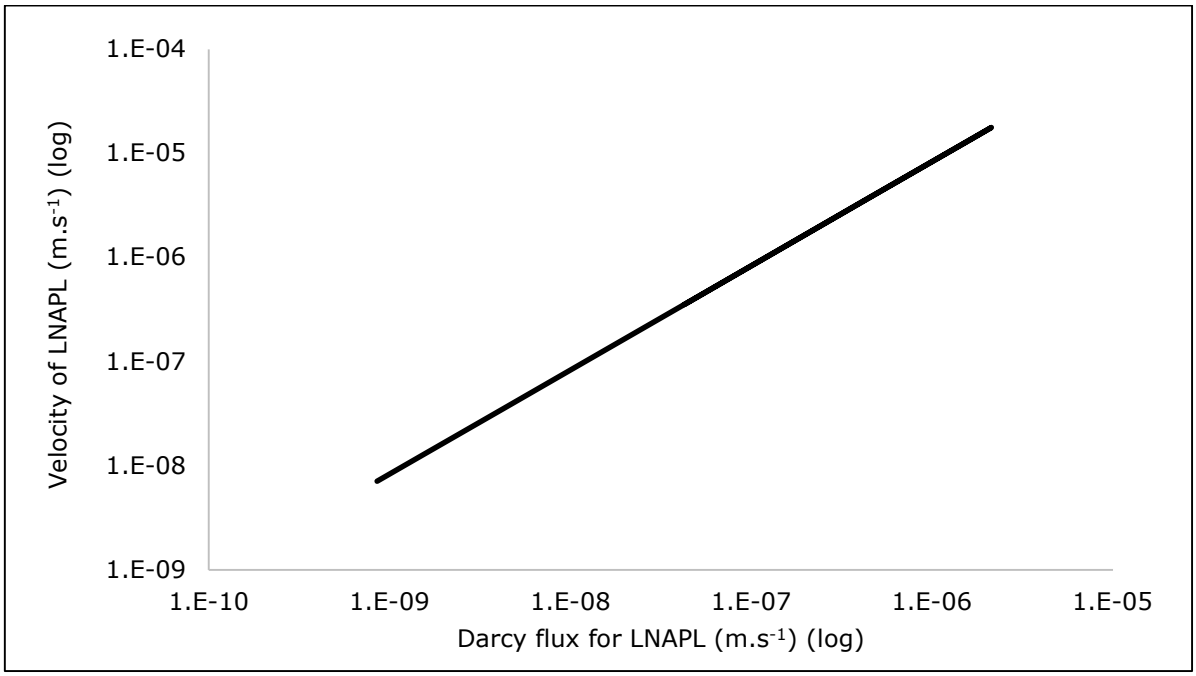

Figure A4-13. Sensitivity of velocity of LNAPL to Darcy flux for LNAPL

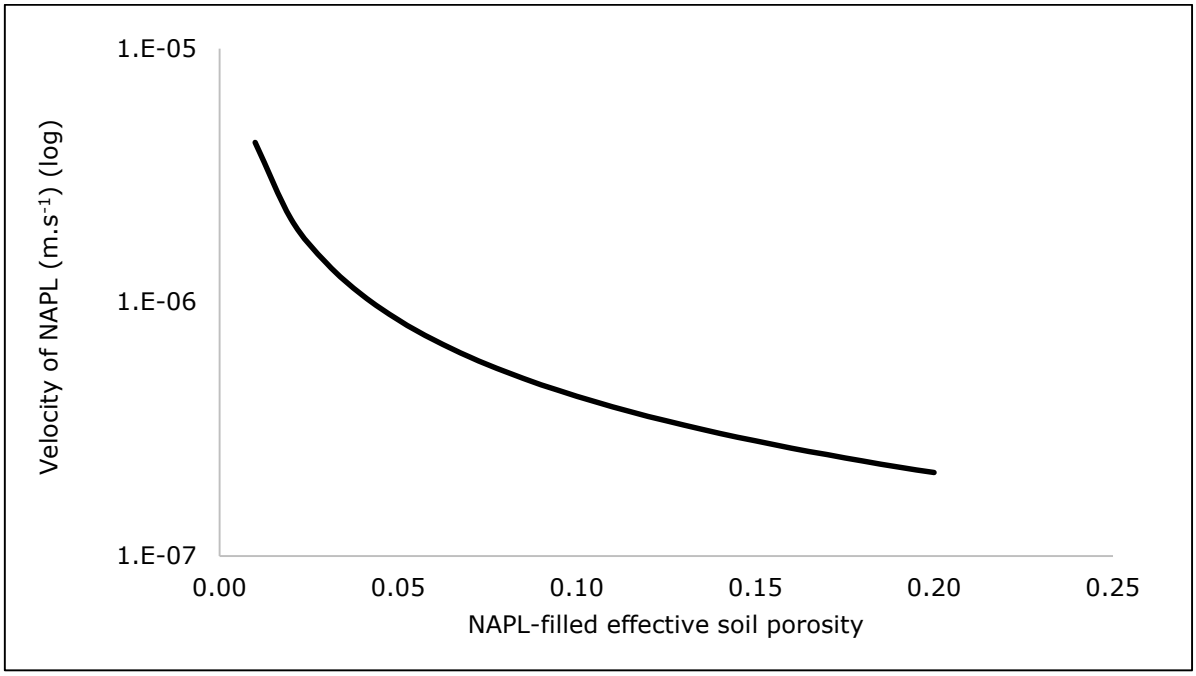

Figure A4-14. Sensitivity of velocity of LNAPL to Darcy flux for LNAPL-filled effective soil porosity

Table A4-4 LNAPL migration rate (2)

CALCULATED PARAMETER	EQUATION	PARAMETER	UNIT	SYMBOL	DEFAULT VALUE
Migration rate	$V_N = \frac{q_N}{\eta S_N}$	**Velocity of LNAPL**	$m.s^{-1}$	v_N	3.55E-07
		Darcy flux for LNAPL	$m.s^{-1}$	q_N	4.26E-08
		Total porosity	-	η	0.4
		NAPL saturation	-	S_N	0.3

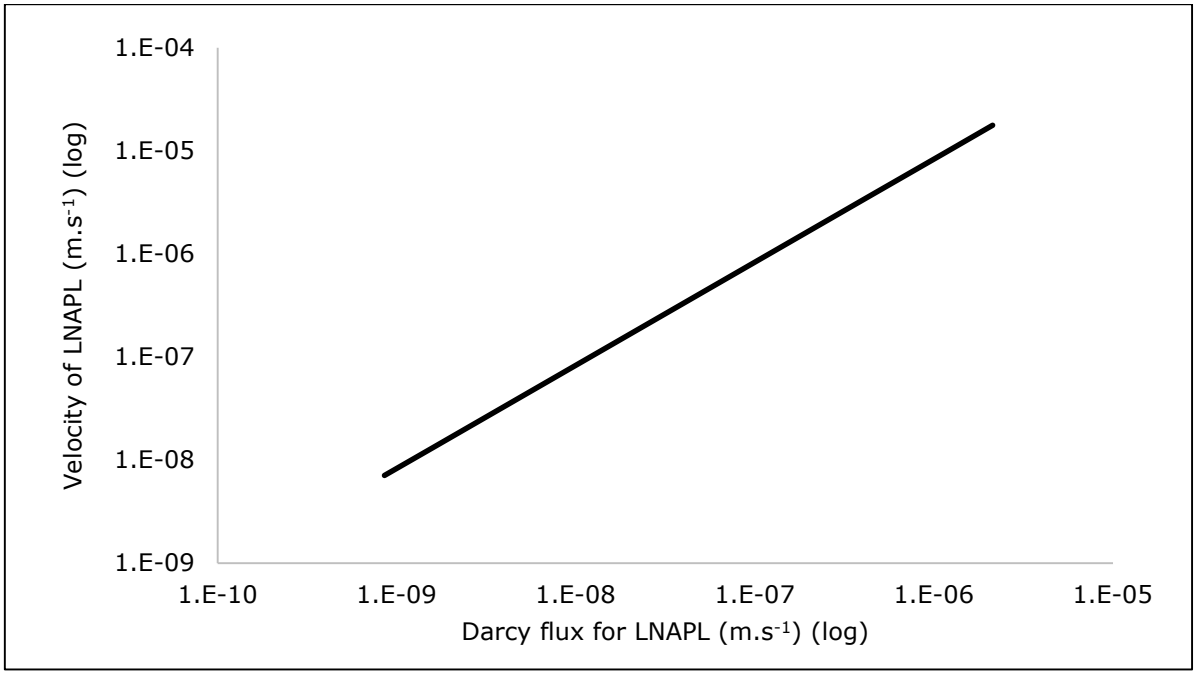

Figure A4-15. Sensitivity of velocity of LNAPL to LNAPL Darcy flux

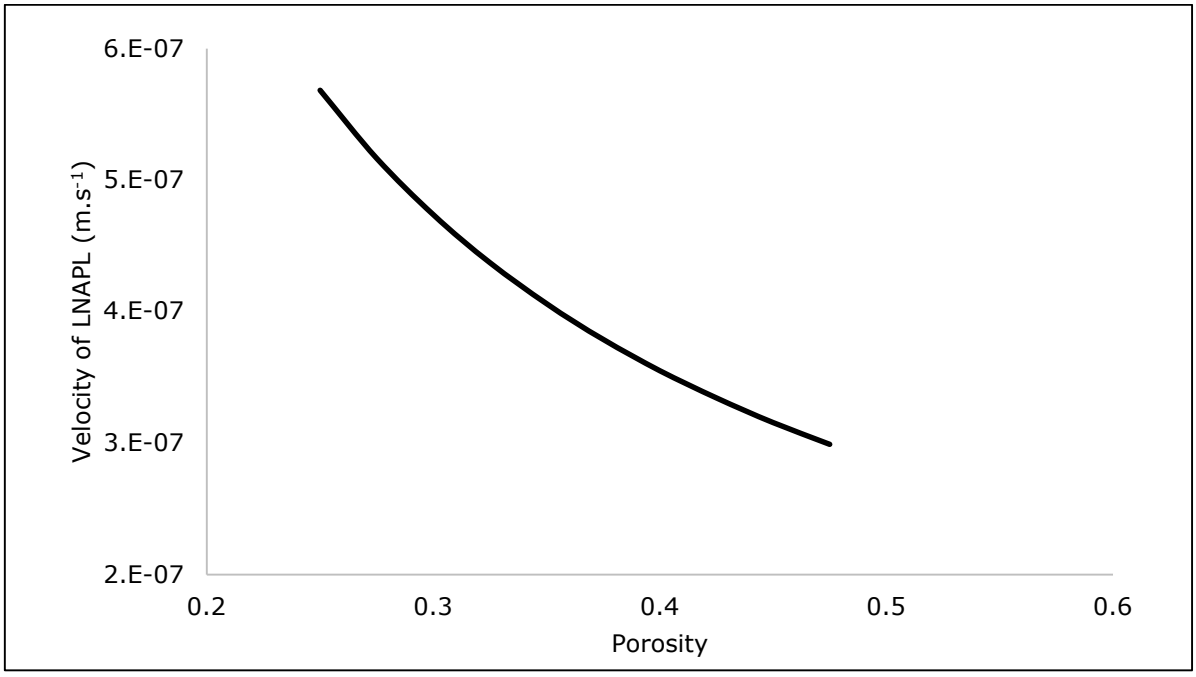

Figure A4-16. Sensitivity of velocity of LNAPL to porosity

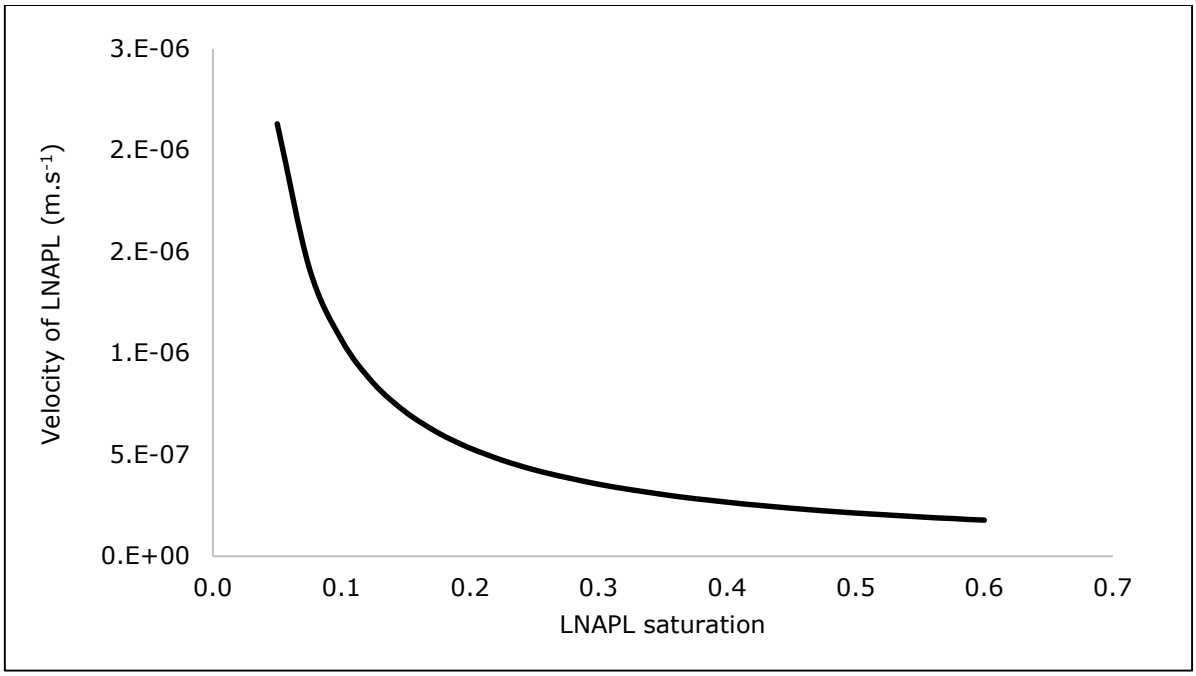

Figure A4-17. Sensitivity of velocity of LNAPL to LNAPL saturation

Table A4-5 Darcy flux for LNAPL

CALCULATED PARAMETER	EQUATION	PARAMETER	UNIT	SYMBOL	DEFAULT VALUE
Migration rate	$q_N = K_N i_N$	**Darcy flux for LNAPL**	$m.s^{-1}$	q_N	4.3E-08
		LNAPL hydraulic conductivity	$m.s^{-1}$	K_N	5.1E-06
		LNAPL gradient	-	i_N	8.3E-03

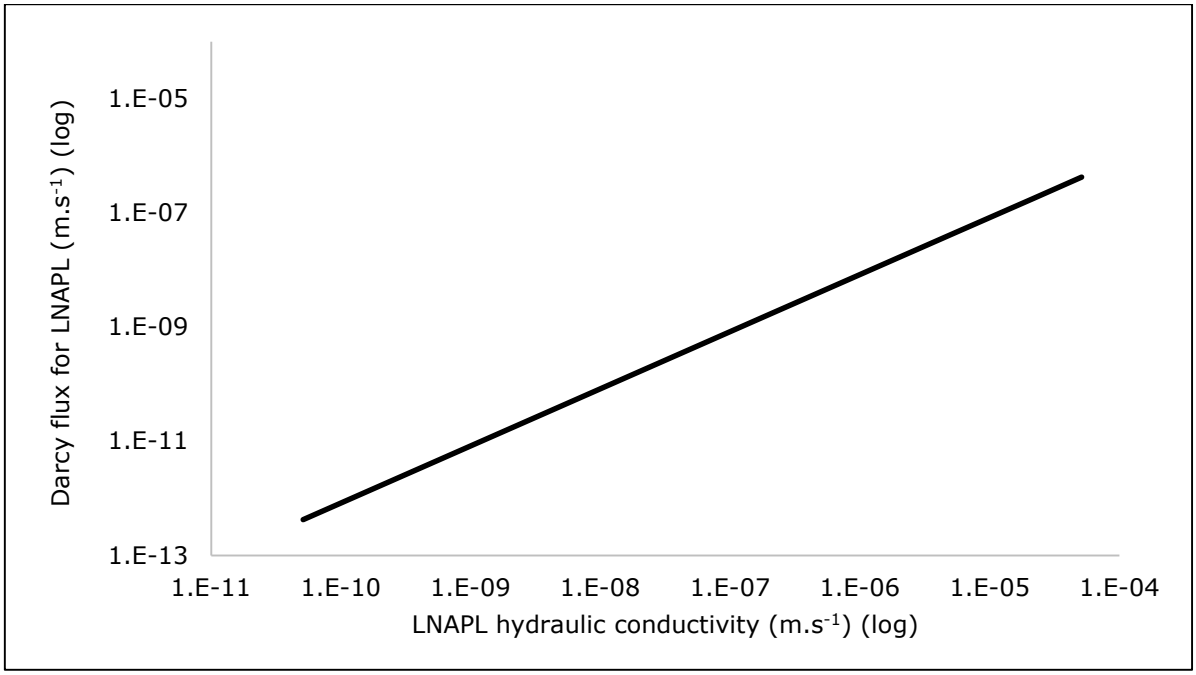

Figure A4-18. Sensitivity of LNAPL Darcy flux to LNAPL hydraulic conductivity

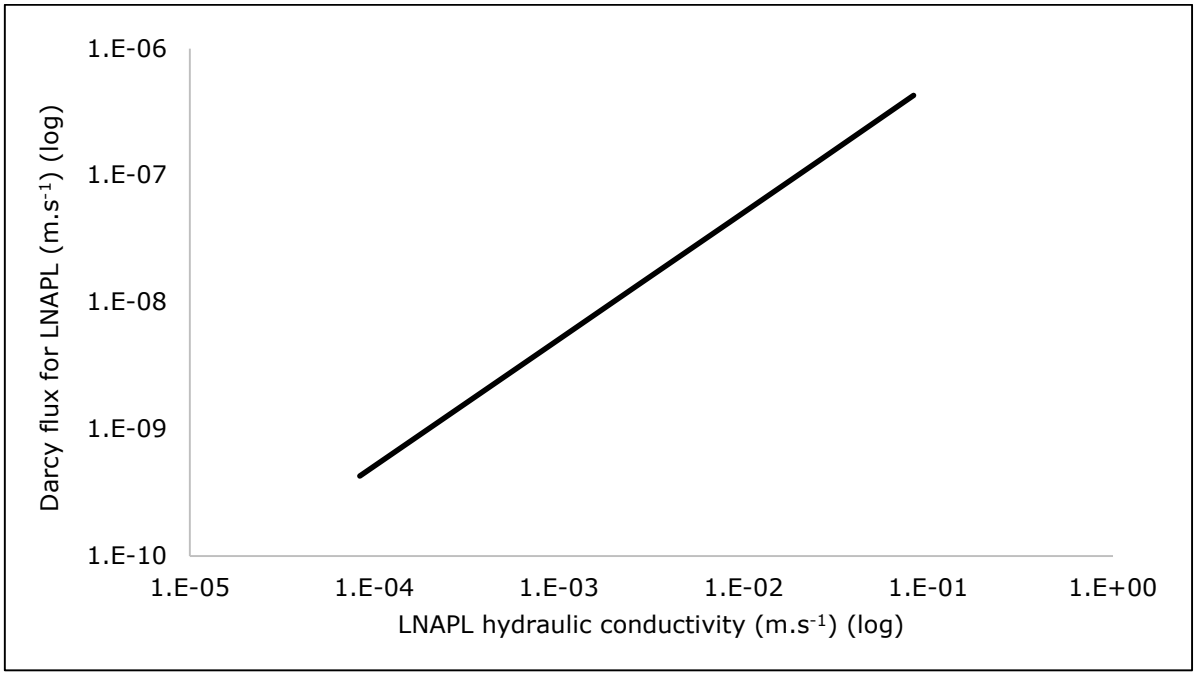

Figure A4-19. Sensitivity of LNAPL Darcy flux to LNAPL hydraulic conductivity

Table A4-6 LNAPL hydraulic conductivity

CALCULATED PARAMETER	EQUATION	PARAMETER	UNIT	SYMBOL	DEFAULT VALUE
Migration rate	$K_N = K_{W\,SAT}\frac{\rho_N}{\rho_W}\frac{\mu_W}{\mu_N}K_{rN}$	**LNAPL hydraulic conductivity**	$m.s^{-1}$	K_N	1.5E-05
		Groundwater hydraulic conductivity for fully saturated condition	$m.s^{-1}$	$K_{W\,SAT}$	1.0E-04
		Density of LNAPL	$kg.m^{-3}$	ρ_N	8.7E+02
		Density of groundwater	$kg.m^{-3}$	ρ_W	1.0E+03
		Dynamic viscosity of LNAPL	Pa.s	μ_N	5.9E-04
		Dynamic viscosity of groundwater	Pa.s	μ_W	1.0E-03
		LNAPL relative permeability	-	k_{rN}	1.0E-01

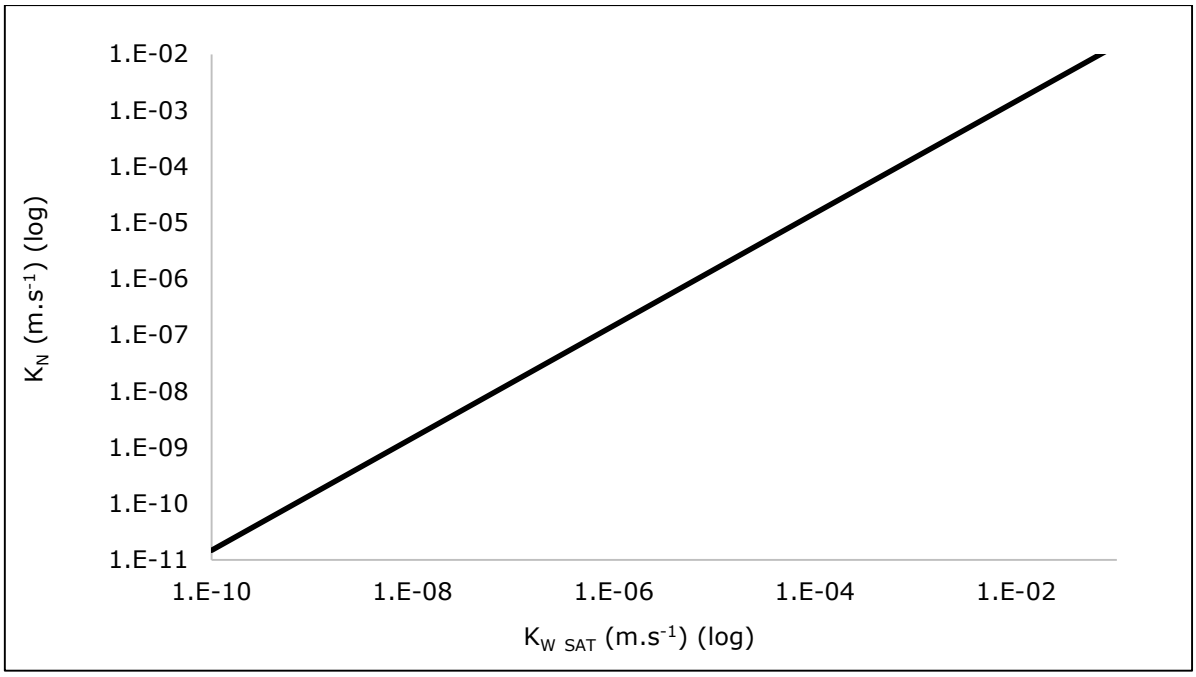

Figure A4-20. Sensitivity of LNAPL hydraulic conductivity to groundwater hydraulic conductivity

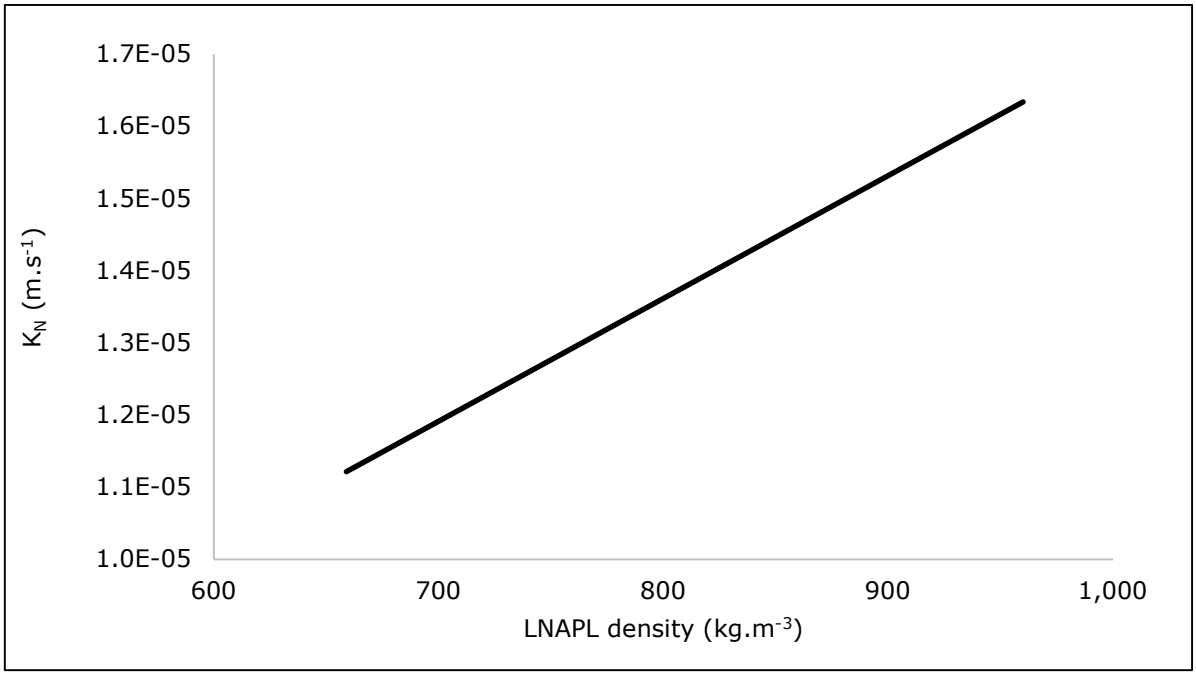

Figure A4-21. Sensitivity of LNAPL hydraulic conductivity to LNAPL density

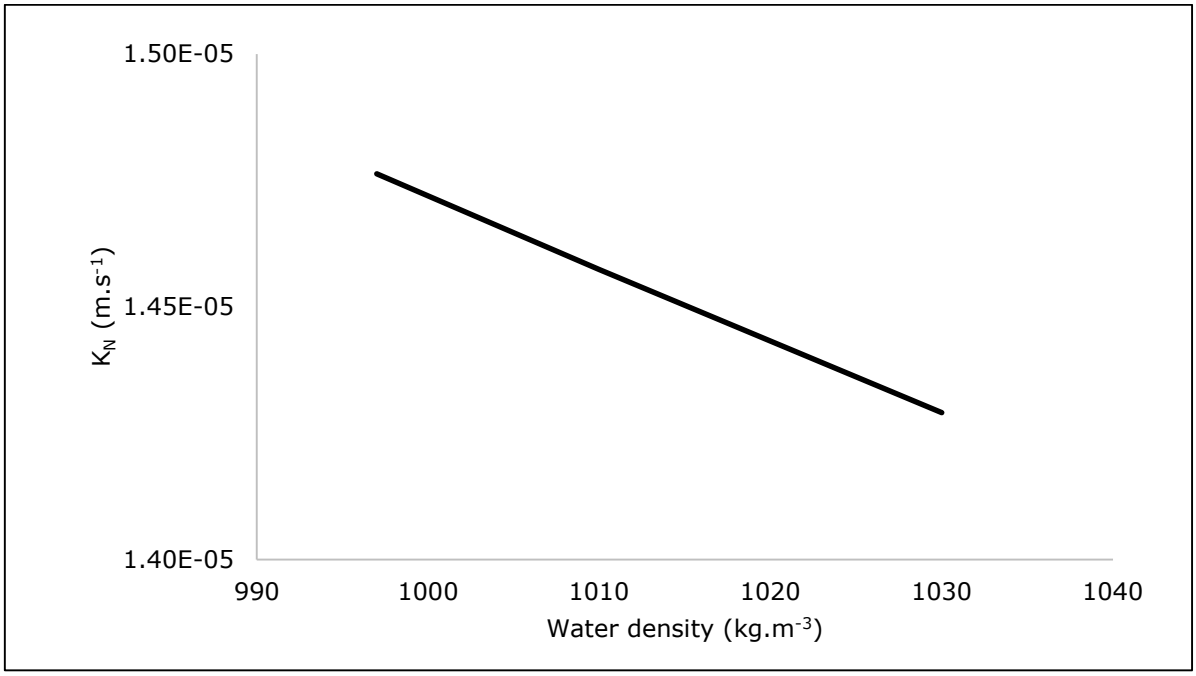

Figure A4-22. Sensitivity of LNAPL hydraulic conductivity to groundwater density

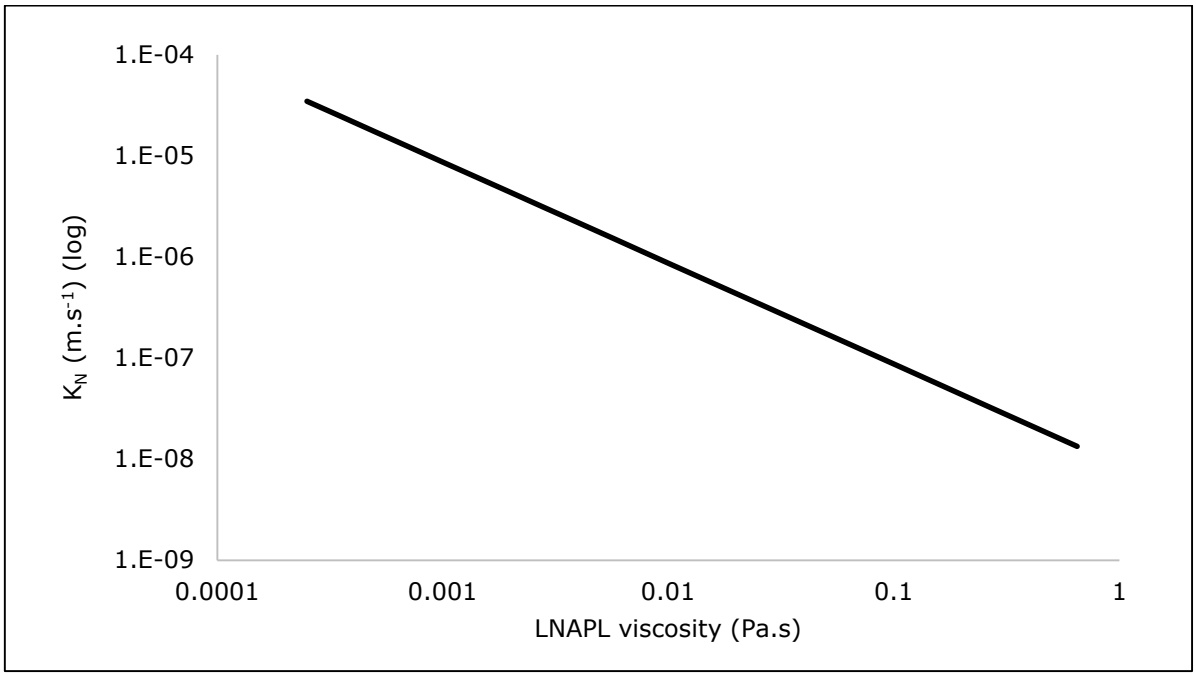

Figure A4-23. Sensitivity of LNAPL hydraulic conductivity to LNAPL viscosity

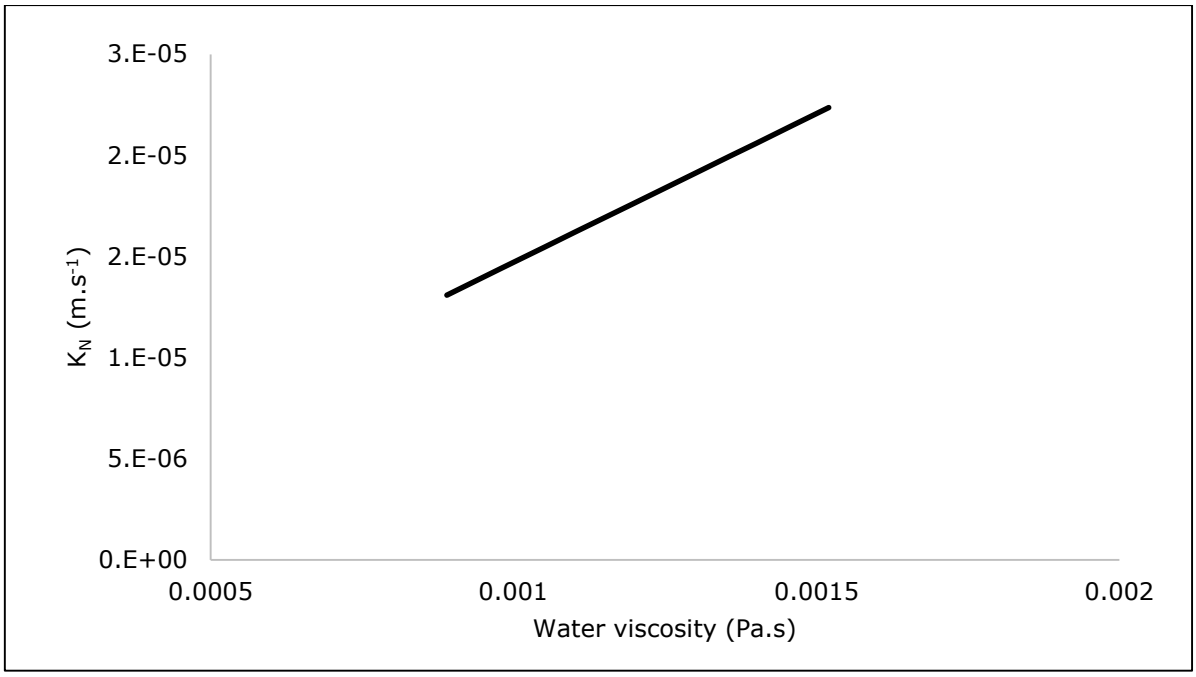

Figure A4-24. Sensitivity of LNAPL hydraulic conductivity to groundwater viscosity

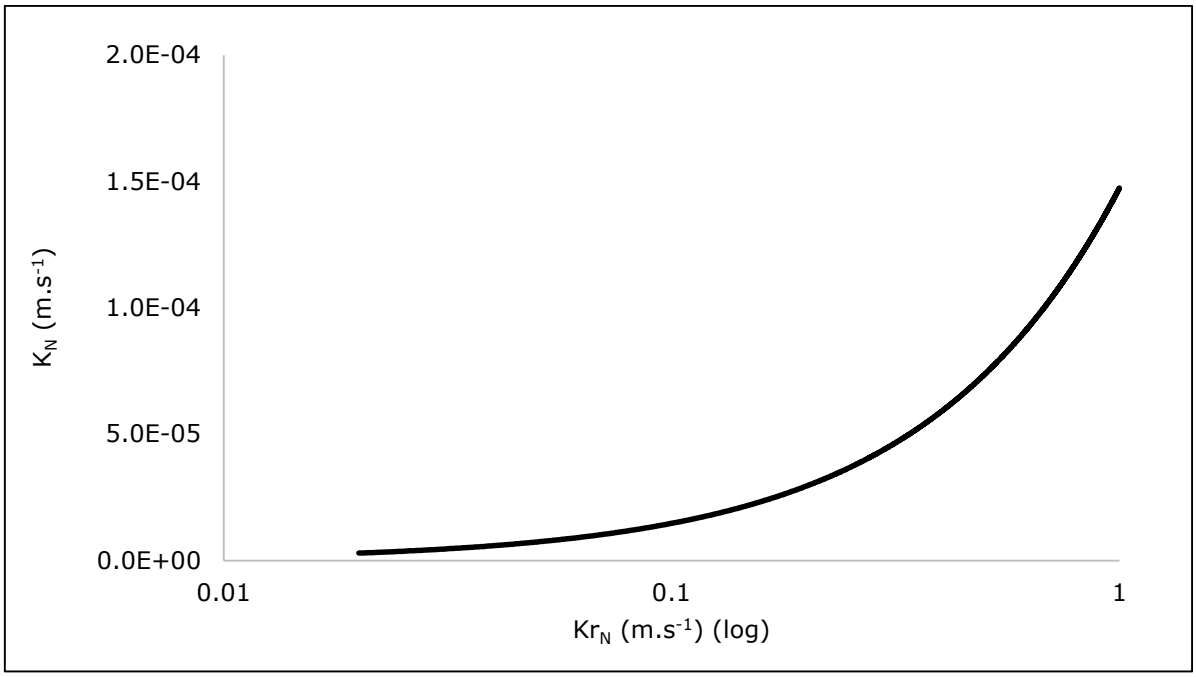

Figure A4-25. Sensitivity of LNAPL hydraulic conductivity to LNAPL relative conductivity

Table A4-7 LNAPL saturation

CALCULATED PARAMETER	EQUATION	PARAMETER	UNIT	SYMBOL	DEFAULT VALUE
LNAPL Saturation	$S_n = \frac{\rho_B . TPH}{\rho_N \eta (10^6)}$	**LNAPL Saturation of pore space**	-	S_n	0.02
		Soil bulk density	kg.m^{-3}	ρ_B	1800
		LNAPL Density	kg.m^{-3}	ρ_N	970
		TPH concentration	mg.kg^{-1}	*TPH*	3659
		Porosity	-	η	0.3

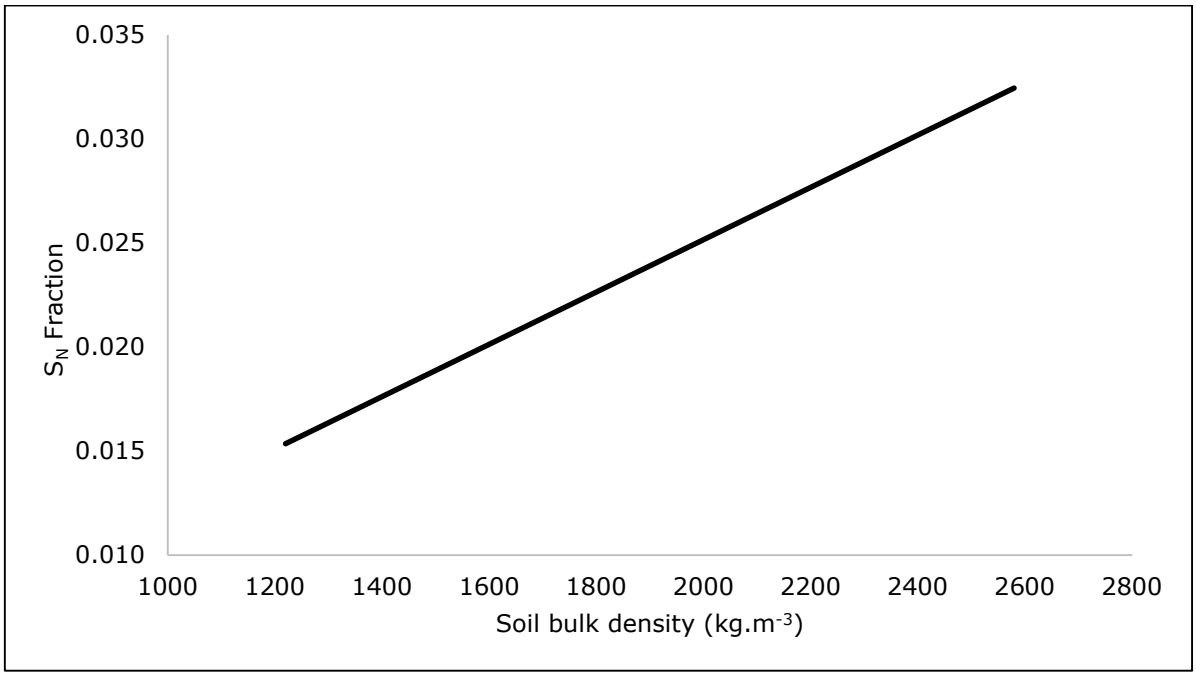

Figure A4-26. Sensitivity of LNAPL saturation to soil bulk density

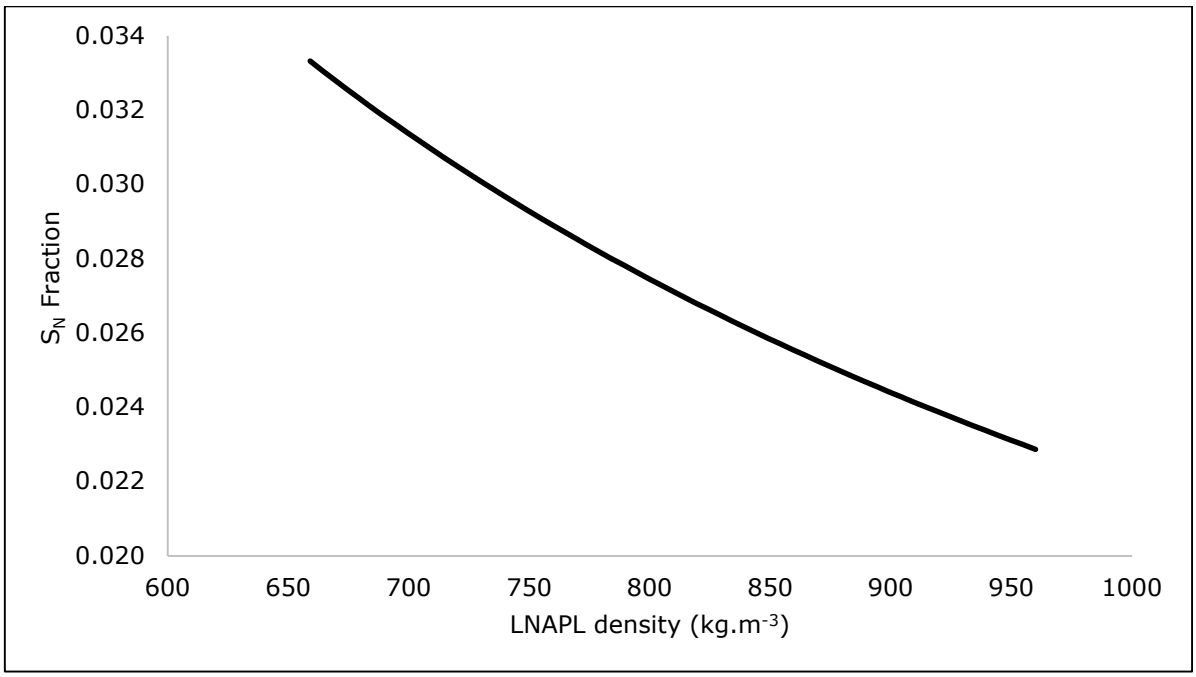

Figure A4-27. Sensitivity of LNAPL saturation to LNAPL density

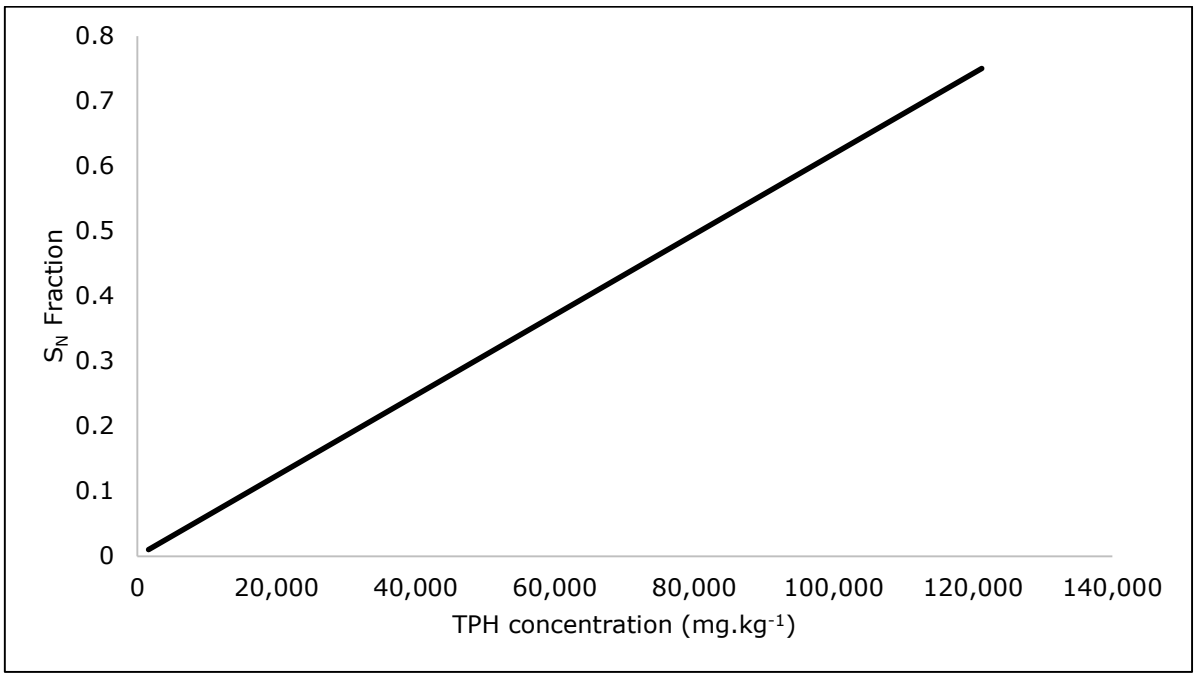

Figure A4-28. Sensitivity of LNAPL saturation to TPH concentration

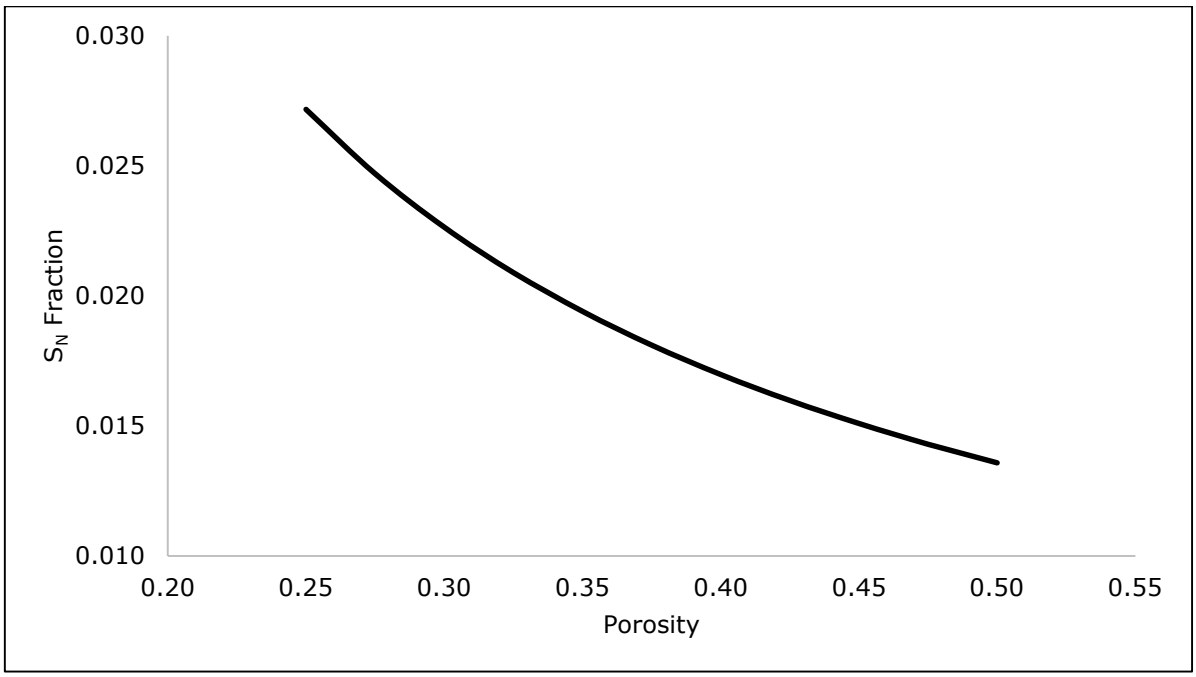

Figure A4-29. Sensitivity of LNAPL saturation to porosity

Calculated parameter	Equation	Parameter	Unit	Symbol	Default value	Input Parameter range	Input Parameter Minimum	Input Parameter maximum	Parameter range justification	Calculated parameter absolute variation (max - min)	Calculated parameter relative variation (max / min)	Qualitiative Parameter Sensitivity	Relative effect over range (Max - min)	Relative effect over range (max / min)	Notes about sensitivity
Depth of LNAPL penetration below the water table (m)	$h_p = \frac{\rho_W g h_n - \left(\frac{2\sigma cos\theta_A}{r}\right)}{\rho_W g}$	**Penetration depth of LNAPL**	m	h_p	5.81	-	-	-	-	-	-	-	-	-	High: > 1 m; Moderate: > 0.5 m; Low: < 0.2 m; Very Low: < 0.1 m for both the LNAPL penetration depth and LNAPL lateral spread
		LNAPL height above water table (m)	m	h_N	8	15	1	16	Site specific	10.96	16.68	High	1.00	0.03	
		Density of LNAPL (kg/m3)	kg.m^3	ρ_N	729	301	659	960	Hexane[1] to greatest measured parameter	2.41	1.46	High	0.22	0.00	
		Density of groundwater	kg.m^3	ρ_W	998	33	997	1030	Water at 25° to seawater at 10°C[1]	0.19	1.03	Low	0.02	0.00	
		Advancing contact angle through the wetting phase	°	θ_A	30	135	20	155	Represents water-wet to NAPL-wet soils[2]	0.07	1.01	Very Low	0.01	0.00	
		Interfacial tension between LNAPL and water	N.m	σ	0.018	0.04	0.01	0.05	Lowest measured value to a high literature value[3]	0.07	1.01	Very Low	0.01	0.00	
		Average pore throat radius	m	r	0.0001	1.69E-05	5E-07	1.75E-05	Equation intersects zero at approximately 5.45E-7 ° for default values*	5.83	513.72	High	0.53	1.00	
		Gravitational force	m.s^2	g	9.81	-	-	-	-	-	-	-	-	-	
LNAPL lateral spread	$h_{NBM,critical} = \left(\frac{\sigma_{NW}}{1-\frac{\rho_N}{\rho_W}} \cdot \frac{\sigma_{AN}}{\frac{\rho_N}{\rho_W}}\right) \frac{h_D}{\sigma_{AW}}$	**Thickness of LNAPL in a well/borehole to exceed pore entry pressure**	m	$h_{NBM,critical}$	0.57	-	-	-	-	-	-	-	-	-	
		Interfacial tension between LNAPL and groundwater	N.m	σ_{NW}	0.02	0.04	0.01	0.05	ref. 3	1.67	9.54	High	0.62	0.21	
		Surface tension of LNAPL	N.m	σ_{AN}	0.03	0.03	0.02	0.05	Lowest to highest literature value[5]	0.19	1.40	Low	0.07	0.03	
		Surface tension of groundwater	N.m	σ_{AW}	0.07	0.01	0.03	0.04	Based on influence of butanol and highest measured seawater value[6,7], but likely to be less sensitive if no co-solvent is present[15]	0.85	2.59	Moderate	0.31	0.06	
		Density of LNAPL	kg.m^3	ρ_N	867	339	659	998	Hexane[1] to greatest measured parameter	2.38	45.08	High	0.88	1.00	
		Density of groundwater	kg.m^3	ρ_W	998	33.00	997.00	1030.00	Water at 25° to seawater at 10°C[1]	0.14	1.32	Low	0.05	0.03	
		Displacement pressure head (i.e., height of capillary fringe)	m	h_D	0.40	1.90	0.10	2.00	Site specific. Can be calculated from a vapour intrusion model[14]	2.71	20.00	High	1.00	0.44	
Migration rate	$V_N = \frac{-q_N}{\eta_{NEff}}$	**Velocity of LNAPL**	m.s^1	v_N	3.6E-07	-	-	-	-	-	-	-	-	-	The outputs of these equations are intrinsically low numbers and so in absolute terms may not appear meaningful. However, the outputs range over orders of magnitude and this has informed the sensitivity judgement
		Darcy flux for LNAPL	m.s^1	q_N	4.3E-08	2.1E-06	8.5E-10	2.1E-06	Site specific	1.8E-05	2500	Moderate	1.00	1.00	
		NAPL-filled Effective porosity	-	η_{NEff}	1.2E-01	0.19	0.01	0.2	Site specific	4.0E-06	20	Low	0.23	0.01	
	$V_N = \frac{q_N}{\eta S_N}$	**Velocity of LNAPL**	m.s^1	v_N	3.55E-07	-	-	-	-	-	-	-	-	-	
		Darcy flux for LNAPL	m.s^1	q_N	4.26E-08	2.1E-06	8.5E-10	2.1E-06	Site specific	1.8E-05	2500	High	1.00	1.00	
		Total porosity	-	η	0.4	0.25	0.25	0.5	Range from literature[8]	2.8E-07	2	Moderate	0.02	0.00	
		NAPL saturation	-	S_N	0.3	0.55	0.05	0.6	Site specific	2.0E-06	12	Low	0.11	0.00	
	$q_N = K_N i_N$	**Darcy flux for LNAPL**	m.s^1	q_N	4.3E-08	-	-	-	-	-	-	-	-	-	
		LNAPL hydraulic conductivity	m.s^1	K_N	5.1E-06	5.1E-05	5.1E-11	5.1E-05	Site specific	4.26E-07	1000000	Very high	1.00	1.00	
		LNAPL gradient	-	i_N	8.3E-03	8.3E-02	8.3E-05	8.3E-02	Site specific	4.26E-07	1000	High	1.00	0.00	
	$K_N = K_{W\,SAT} \frac{\rho_N}{\rho_W} \frac{\mu_W}{\mu_N} k_{rN}$	**LNAPL hydraulic conductivity**	m.s^1	K_N	1.5E-05	-	-	-	-	-	-	-	-	-	
		Groundwater hydraulic conductivity for fully saturated condition	m.s^1	$K_{W\,SAT}$	1.0E-04	0.10	1E-10	1.00E-01	Range from literature[9]	1.5E-02	1000000000	Very High	1.00	1.00	
		Density of LNAPL	kg.m^3	ρ_N	8.7E+02	301	659	960	Hexane[1] to greatest measured parameter	5.1E-06	1.46	Low	0.00	0.00	
		Density of groundwater	kg.m^3	ρ_W	998	33	997	1030	ref. 1	4.7E-07	1.03	-	0.00	0.00	
		Dynamic viscosity of LNAPL	Pa.s	μ_N	5.9E-04	0.65	0.0003	0.65	From diethyl ether[1] to highest recorded in the field	3.5E-05	2600	Moderate	0.002	0.00	
		Dynamic viscosity of groundwater	Pa.s	μ_W	1.0E-03	0.0006	0.00089	0.00152	Based on temperature range from 5 to 25°C[10]	9.3E-06	2	-	0.00	0.00	
		LNAPL relative permeability	-	k_{rN}	1.0E-01	0.95	5.00E-02	1.00	Site specific	1.4E-04	20	High	0.01	0.00	
NAPL Saturation	$S_n = \frac{\rho_B TPH}{\rho_N \eta (10^6)}$	**LNAPL Saturation of pore space**	-	S_n	0.02	-	-	-	-	-	-	-	-	-	The NAPL saturation is mainly affected by the TPH value
		Soil bulk density	kg.m^3	ρ_B	1800	1360	1220	2580	ref. 12	0.02	2.1	Low	0.02	0.03	
		LNAPL Density	kg.m^3	ρ_N	970	301	659	960	Hexane[1] to greatest measured parameter	0.01	1.46	Low	0.01	0.02	
		TPH concentration	mg.kg	TPH	3659	119633.4	1616.6	121250	Site specific	0.74	75	High	1.00	1.00	
		Porosity	-	η	0.3	0.25	0.25	0.5	ref. 8	0.01	2	Low	0.02	0.03	

	References	Notes
1	CRC Handbook of Chemistry and Physics, 95th Edition, ed. Haynes, W.M. 2014.	Hexane at 20°c
2	Al-Futaisi, A. and Patzek, T.W., 2004. Secondary imbibition in NAPL-invaded mixed-wet sediments. *Journal of contaminant hydrology*, *74*(1-4), pp.61-81.	
3	Chang, L.C., Chen, H.H., Shan, H.Y. and Tsai, J.P., 2009. Effect of connectivity and wettability on the relative permeability of NAPLs. *Environmental geology*, *56*(7), pp.1437-1447.	
4	Gao, Z. and Hu, Q., 2013. Estimating permeability using median pore-throat radius obtained from mercury intrusion porosimetry. *Journal of Geophysics and Engineering*, *10*(2), p.025014.	Data for environmentally-relevent soils are sparse and values are typically derrived for oil-producting low-permeability rocks. The highest value in ref4 is 0.000001 m - 100 times smaller than the equation default value. The CL:AIRE 2014 LNAPL handbook uses an assumed value.
5	Egemen, E., Nirmalakhandan, N. and Trevizo, C., 2000. Predicting surface tension of liquid organic solvents. *Environmental science & technology*, *34*(12), pp.2596-2600.	2,2-Dimethylbutane to Adiponitrile
6	Bikerman (1970) in: Smith, J.E. and Gillham, R.W., 1999. Effects of solute concentration–dependent surface tension on unsaturated flow: Laboratory sand column experiments. *Water Resources Research*, *35*(4), pp.973-982.	Assuming up to 6% butanol concentration: alcohols lower the surface tension of water and can often be co-contaminants at NAPL sites (author's personal experience)
7	Nayar, K.G., Panchanathan, D., McKinley, G.H. and Lienhard, J.H., 2014. Surface tension of seawater. *Journal of Physical and Chemical Reference Data*, *43*(4), p.043103.	The maximum surface tension of seawater is given as 0.0078 N/m
8	Carnica, J.N., 1995. *Geotechnical engineering: soil mechanics*.	
9	Hillel, D., 2003. *Introduction to environmental soil physics*. Elsevier.	
10	Ritzema, H.P., 2006. *Drainage principles and applications* (No. 16). ILRI.	
11	https://www.engineeringtoolbox.com/dirt-mud-densities-d_1727.html, 14/04/2020	
12	Harter, T., Publication 8083, From Harter, T., 2003 *Basic concepts of groundwater hydrology*. UCANR Publications.	Groundwater velocity can be effectively zero so only an upper limit was referenced
13	MacKay, A.A. and Gschwend, P.M., 2001. Enhanced concentrations of PAHs in groundwater at a coal tar site. *Environmental science & technology*, *35*(7), pp.1320-1328.	
14	US Environmental Protection Agency. Documentation for EPA's implemetnaion of the Johnson and Ettinger Model to Evaluate Site Specific Vapor Intrusion into Buildings. Version 6. 2017.	